



Published in final edited form as:

J Med Chem. 2012 January 12; 55(1): 342–356. doi:10.1021/jm201229j.

Structure-Activity Relationships of Truncated C2- or C8-Substituted Adenosine Derivatives as Dual Acting A_{2A} and A₃ Adenosine Receptor Ligands

Xiyun Hou¹, Mahesh S. Majik¹, Kyunglim Kim¹, Yuna Pyee², Yoonji Lee¹, Varughese Alexander¹, Hwa-Jin Chung², Hyuk Woo Lee¹, Girish Chandra¹, Jin Hee Lee¹, Seul-gi Park¹, Won Jun Choi^{1,3}, Hea Ok Kim¹, Khai Phan⁴, Zhan-Guo Gao⁴, Kenneth A. Jacobson⁴, Sun Choi¹, Sang Kook Lee², and Lak Shin Jeong^{1,*}

¹Laboratory of Medicinal Chemistry, College of Pharmacy and Department of Bioinspired Science, Ewha Womans University, Seoul 120-750, Korea

²College of Pharmacy, Seoul National University, Seoul 151-742, Korea

³College of Pharmacy, Dongguk University, Kyungki-do 410-774, Korea

⁴Molecular Recognition Section, Laboratory of Bioorganic Chemistry, National Institute of Diabetes, and Digestive and Kidney Disease, National Institutes of Health, Bethesda, Maryland 20892, USA

Abstract

Truncated N⁶-substituted-4'-oxo- and 4'-thioadenosine derivatives with C2 or C8 substitution were studied as dual acting A_{2A} and A₃ adenosine receptor (AR) ligands. The lithiation-mediated stannyl transfer and palladium-catalyzed cross coupling reactions were utilized for functionalization of the C2 position of 6-chloropurine nucleosides. An unsubstituted 6-amino group and a hydrophobic C2 substituent were required for high affinity at the hA_{2A}AR, but hydrophobic C8 substitution abolished binding at the hA_{2A}AR. However, most of synthesized compounds displayed medium to high binding affinity at the hA₃AR, regardless of C2 or C8 substitution, and low efficacy in a functional cAMP assay. Several compounds tended to be full hA_{2A}AR agonists. C2 substitution probed geometrically through hA_{2A}AR-docking, was important for binding in order of hexenyl > hexenyl > hexanyl. Compound **4g** was the most potent ligand acting dually as hA_{2A}AR agonist and hA₃AR antagonist, which might be useful for treatment of asthma or other inflammatory diseases.

Keywords

lithiation-mediated stannyl transfer; structure-activity relationship; adenosine receptors; truncated adenosine; palladium-catalyzed cross coupling; dual-acting ligands

*To whom correspondence should be addressed: Lak Shin Jeong, Ph.D., Laboratory of Medicinal Chemistry, College of Pharmacy and Department of Bioinspired Science, Ewha Womans University, Seoul 120-750, Korea, Tel) 82-2-3277-3466, Fax) 82-2-3277-2851, lakjeong@ewha.ac.kr.

Supporting Information Available: Scheme 1S for the mechanism of lithiation mediated stannyl transfer for the formation of **7**. This material is available free of charge via the Internet at <http://pubs.acs.org>.

Introduction

The structure of endogenous adenosine, which binds to four subtypes (A_1 , A_{2A} , A_{2B} , and A_3) of adenosine receptors (ARs)^{1,2} to induce physiological effects, has been extensively modified, particularly on N^6 and/or 4'-hydroxymethyl positions for the development of potent and selective AR ligands.^{3,4} Among these, 2-chloro- N^6 -(3-iodobenzyl)-5'- N -methylcarbamoyladenine (Cl-IB-MECA, **1a**, X = O, R = 3-iodobenzyl; K_i = 1.0 nM for hA_3AR) is a versatile A_3AR agonist, which is in clinical trial as an anticancer agent (Figure 1).⁵ 2-Chloro- N^6 -(3-iodobenzyl)-5'- N -methylcarbamoyl-4'-thioadenosine (thio-Cl-IB-MECA, **1b**, X = S, R = 3-iodobenzyl; K_i = 0.38 nM for hA_3AR), which has a bioisosteric relationship to **1a** was also found to be a potent and selective A_3AR agonist.⁶ Compounds **1a** and **1b** showed anti-proliferative effects in various cancer cell lines, resulting from down-regulation of the Wnt signaling pathway and other mechanisms.⁷

Recently, truncated C2- or C8-substituted 4'-thioadenosine derivatives **3** containing an appended hydrophobic hexenyl or hexynyl chain at the C2 or C8 position of **2** were designed and synthesized.¹¹ Among these, a C2-hexynyl derivative **3** (R = hexynyl) was discovered as a new template (K_i = 7.19 ± 0.6 nM) for the development of potent $A_{2A}AR$ agonists¹² while maintaining antagonism at the A_3AR (K_i = 11.8 ± 1.3 nM).¹¹ However, C8-substituted derivatives displayed greatly reduced binding affinity at the $A_{2A}AR$, while maintaining high affinity at the A_3AR , indicating that the binding pocket for C8 substituents in the $A_{2A}AR$ was relatively small, when compared with that for C2 substituents, which could accommodate steric bulk in both A_{2A} and A_3AR s.¹¹ This dual activity at both of these subtypes might be beneficial for developing therapeutic drugs against diseases such as asthma and inflammation.

Thus, it was of great interest to extend the structure-activity relationship study of the truncated 4'-thio series **3** to the 4'-oxo series **4** with various substituents at C2 or C8 positions. Truncated 4'-oxo adenosine derivatives containing C2-H or C2-Cl were previously found to interact potently and selectively with the A_3AR .^{9c,9d} It was also interesting to determine the effects of N^6 substituents on binding affinity to the $A_{2A}AR$, because 3-halobenzyl substituents at the N^6 position generally increased the binding affinity and selectivity at the A_3AR .^{3,4} Herein, we report a full account of truncated C2-, C8-, or N^6 -modified adenosine derivatives acting dually at the A_{2A} and A_3AR s.

Results and discussion

Chemistry

First, 2-hexynyl- N^6 -substituted-adenosine derivatives **4a-f** were synthesized from glycosyl donor **5**,⁹ which was easily synthesized from commercially available 2,3-*O*-isopropylidene-D-erythronic γ -lactone in two steps, as shown in Scheme 1.

Condensation of glycosyl donor **5** with silylated 6-chloropurine in the presence of trimethylsilyl trifluoromethanesulfonate (TMSOTf) as a Lewis acid yielded the β -anomer **6**^{9c} (71%) as a single diastereomer. The anomeric configuration in **6** was easily confirmed by a ¹H NMR nuclear Overhauser effect (NOE) experiment between H-8 and 3'-H. For the functionalization at the C2 position of 6-chloropurine in **6**, lithiation-mediated stannyl transfer of 6-chloropurine nucleosides reported by Tanaka and coworkers^{13a} was utilized. Treatment of **6** with a freshly prepared lithium 2,2,6,6-tetramethylpiperidide (LiTMP) initially formed the C8-lithiated species, because the C8-hydrogen is more acidic than the C2-hydrogen. Reaction of the C8-lithiated species with *n*-tributyltin chloride produced C2-stannyl derivative **7** as a sole regioisomer, which resulted from an anionic transfer of the stannyl group from C8 to the C2 position (see Scheme 1S in the Supporting Information for

a reaction mechanism).^{13a} Treatment of **7** with iodine gave 2-iodo-6-chloropurine derivative **8**.¹³ Sonogashira¹⁴ coupling of **8** with 1-hexyne in the presence of tetrakis(triphenylphosphine)palladium and cesium carbonate yielded C2-hexynyl derivative, which was hydrolyzed with 1 *N* HCl to give the 2-hexynyl-6-chloro derivative **9**. Compound **9** was converted into 2-hexynyl-adenosine derivative **4a** and 2-hexynyl-*N*⁶-substituted-adenosine derivatives **4b–e** by treatment with ammonia and 3-halobenzyl amines, respectively. 2-Hexynyladenosine derivative **4a** was subjected to hydrogenation with 10% Pd on carbon to give saturated analogue **4f**.

The corresponding 4'-thioadenosine derivatives **4g–k** were synthesized from glycosyl donor **10**, which was easily synthesized from D-mannose according to our previously published procedure,⁹ as illustrated in Scheme 2.

The lithiation-mediated stannyl transfer¹³ of 6-chloropurine nucleosides used in Scheme 1 was first tried for the synthesis of 4'-thioadenosine derivatives **4g–k**, but resulted in poor formation of 2-iodo-6-chloropurine derivative **11** (5%), due to the presence of acidic 1' and 4'-protons (conventional nucleoside numbering) in the thiophene ring. Thus alternative method of directly condensing glycosyl donor **10** with freshly prepared 2-iodo-6-chloropurine^{13b} was attempted, as shown in Scheme 2. Condensation of glycosyl donor **10** with silylated 2-iodo-6-chloropurine in the presence of TMSOTf afforded the β -anomer **11** (60%) along with a trace amount of its *a*-anomer. The anomeric configuration was also confirmed by a ¹H NMR NOE experiment between H-8 and 3'-H. Sonogashira¹⁴ coupling reaction of **11** with 1-hexyne in the presence of tetrakis(triphenylphosphine)palladium {(Ph₃P)₄Pd} and cesium carbonate yielded the C2-hexynyl derivative **12**. Treatment of **12** with 1 *N* HCl yielded the 2-hexynyl-6-chloro derivative **13**, which was treated with ammonia and 3-halobenzyl amines to afford 2-hexynyl-4'-thioadenosine derivative **4g**¹¹ and 2-hexynyl-*N*⁶-substituted-4'-thioadenosine derivatives **4h–k**, respectively.

After the successful introduction of the hexynyl group at the C2 position, we decided to extend the synthesis to other hydrophobic C2-hexenyl and C2-hexanyl derivatives. Synthesis of 2-hexenyl derivatives was accomplished using a Suzuki¹⁵ coupling reaction as a key step (Scheme 3). Treatment of 2-iodo-6-chloro derivatives **8** and **11** with methanolic ammonia gave 2-iodo-6-amino derivatives **14** and **15**, respectively. Suzuki coupling of C2-iodo derivatives **14** and **15** with (*E*)-1-catecholboranylhexene,¹⁶ prepared by treating with 1-hexyne and catecholborane in the presence of (Ph₃P)₄Pd, produced 2-hexenyl derivatives **16** and **17**, respectively. Treatment of **16** and **17** with 1 *N* HCl gave 2-hexenyl-adenosine derivative **4l** and 2-hexenyl-4'-thioadenosine derivative **4m**¹¹, respectively.

Using a similar synthetic strategy used in Scheme 1, C8-substituted adenosine derivatives **4n–p** were synthesized from glycosyl donors **5** and **10** (Scheme 4). Condensation of **5**⁹ with silylated 6-chloropurine under Lewis acid conditions, followed by treatment with methanolic ammonia afforded adenine derivative **18**. Treatment of **18** with bromine and sodium acetate in methanol yielded 8-bromo derivative **19**. However, in the case of 4'-thioadenosine derivatives, the same method was tried, but resulted in the extensive decomposition of starting material. Thus, direct condensation of **10** with 8-bromoadenine¹⁷ under Lewis acid conditions provided 8-bromo derivative **20**, but only in 20% yield. Sonogashira coupling of **19** and **20** with 1-hexyne using bis(triphenylphosphine)palladium dichloride {(Ph₃P)₄PdCl₂} gave C8-hexynyl derivatives **21** and **22**, respectively. Treatment of **21** and **22** with 1 *N* HCl yielded the final 8-hexynyl derivatives **4n** and **4o**,¹¹ respectively. Compound **4n** was converted to *n*-hexynyl derivative **4p** using catalytic hydrogenation.

For the synthesis of 8-hexenyl derivatives **4q** and **4r**, 8-bromo derivatives **19** and **20** were coupled with (*E*)-1-catecholboranylhexene¹⁶ under Suzuki conditions¹⁵ to give C2-hexenyl

derivatives **23** and **24**, respectively. Removal of the isopropylidene group in **23** and **24** under acidic conditions afforded the 8-hexenyladenosine derivative **4q** and the 8-hexenyl-4'-thioadenosine derivative **4r**.¹¹

Biological evaluation

Binding assays were carried out using standard radioligands and membrane preparations from Chinese hamster ovary (CHO) cells stably expressing the human (h) A₁ or A₃AR or human embryonic kidney (HEK)-293 cells expressing the hA_{2A}AR.¹⁸ Nonspecific binding was defined using 10 μM of 5'-*N*-ethylcarboxamidoadenosine (**25**, NECA).

As shown in Table 1, 4'-thio derivatives generally exhibited higher binding affinities to hA_{2A} and hA₃ARs than the corresponding 4'-oxo derivatives. In case of *N*⁶-amino derivatives, most of C2-substituted analogues (R₂ = hexynyl and hexenyl) showed moderate to high potent binding affinities at the hA_{2A} and hA₃ARs, while most of C8-substitutions (R₃ = hexynyl, hexenyl, and hexanyl) reduced binding affinity at the hA_{2A}AR, but maintained high affinity at the hA₃AR. These findings indicate that bulky hydrophobic pockets exist in the binding sites of A_{2A}AR and A₃AR, allowing the C2-substituent to form favorable hydrophobic interactions, but a bulky hydrophobic group at C8 position could be tolerated only at the binding site of the hA₃AR, but not hA_{2A}AR. The ability to enhance affinity at the A_{2A}AR in the truncated series by extending an unsaturated carbon chain at the C2 position implies a mode of receptor binding in common with the riboside series.¹⁹ However, introduction of a hydrophobic 3-halobenzyl substituent on the *N*⁶-amino group of **4a** and **4g**, resulting in **4b–4e** and **4h–4k**, respectively dramatically decreased the binding affinity at the hA_{2A}AR, but maintained the binding affinity at the hA₃AR. These results indicate that an unsubstituted primary amino group at the *N*⁶ position is conducive to high binding affinity at the hA_{2A}AR, while a bulky hydrophobic substituent at the *N*⁶ position is essential for high affinity at the hA₃AR. Correlating pharmacological behavior with the nucleoside substitution pattern, a hexynyl substituent generally produced higher binding affinity than the corresponding hexenyl substituent, and two hexanyl derivatives (**4f** and **4p**) were greatly reduced in binding affinity at the three subtypes of hARs, indicating that the geometry of the substituent is important for the binding affinity. All compounds showed weak binding affinity at the hA₁AR, although **4a**, **4n**, and **4q** displayed measurable K_i values less than 1 μM at this subtype. Thus, in some cases hydrophobic substitution at the C8 position permitted moderate binding affinity (K_i < 500 nM) at the hA₁AR. 4'-Oxo derivative **4d** and 4'-thio derivatives **4i**, **4j**, **4k**, and **4o** displayed high selectivity for the hA₃AR in comparison to hA₁AR and hA_{2A}AR, with K_i values in the range of 20 – 67 nM. From the SAR study, compound **4g** was discovered to be the most potent dually acting ligand, binding with high affinity at both the hA_{2A}AR (K_i = 7.19 ± 0.6 nM) and hA₃AR (K_i = 11.8 ± 1.3 nM) to the exclusion of the hA₁AR.¹¹

The functional screening protocol used at the hA₃AR consisted of examining the effects of a single concentration of each compound (10 μM), which in each case except for **4f** and **4p** far exceeded the K_i values in binding and therefore was interpreted as a roughly maximal effect under ligand saturating conditions. As shown in Table 1, most of the derivatives are low efficacy partial agonists at the hA₃AR, with relative percent inhibition of cyclic adenosine-5'-monophosphate (cAMP) formation not exceeding 50%. The 4'-thio C2-substituted derivatives **4i**, **4j**, and **4k** appear to be hA₃AR-selective partial agonists. Some of the C2-substituted derivatives, **4c**, **4h**, **4i**, **4k**, and **4l**, displayed between 40–50% maximal efficacy in comparison to **1a**. This was in contrast to another C2 derivative **4g**, which did not have significant residual efficacy at the hA₃AR. The C8-substituted derivatives **4n** through **4r** did not exceed 25% of the maximal efficacy to **1a**. A C8-hexynyl derivative **4o** in the 4'-thio series, which was highly potent in hA₃AR binding (K_i = 20 nM) and selective in comparison to A₁AR and A_{2A}AR, did not have significant residual efficacy at the hA₃AR.

In a set of full concentration-response experiments, compound **4g** induced parallel right shifts of the concentration-response curve of a full agonist **1a** in the inhibition of cAMP production at the hA₃AR expressed in CHO cells, indicating that it is as a full, competitive antagonist ($K_B = 1.69$ nM) at the hA₃AR,¹¹ as our previously reported truncated N⁶-substituted 4'-thioadenosine derivatives.⁹ Similarly, by the same criteria compound **4m** was a competitive antagonist ($K_B = 23.9$ nM) at the hA₃AR (Figure 2).

However, in a cAMP functional assay at the hA_{2A}AR expressed in CHO cells, several of these nucleoside agonists demonstrated a higher degree of relative efficacy than at the hA₃AR. For example, the most potent compound **4g** behaved as a full agonist compared to the standard CGS21680 and displayed an EC₅₀ of 12 nM,¹¹ and compound **4a** displayed a maximal stimulation of cAMP formation of $89.9 \pm 3.8\%$, relative to the full agonist NECA (= 100%), with an EC₅₀ of 80.3 nM (Figure 3A).

Compounds **4l** and **4m** were also agonists at the hA_{2A}AR, with maximal percent activity at 10 μ M relative to NECA of $83.0 \pm 5.2\%$ and $108.8 \pm 5.1\%$, respectively. In a full concentration-response curve (Figure 3B), compound **4m** displayed an EC₅₀ value of 20.6 ± 1.58 nM in stimulation of cAMP formation via the hA_{2A}AR. As reported by us previously, compound **4g** was a potent full agonist in stimulation of cAMP formation via the hA_{2A}AR with an EC₅₀ of 12 nM.¹¹ The findings that truncated nucleosides **4g** and **4m** serve as dual ligands acting at the hA_{2A} and hA₃ARs are similar to the pharmacological profile of a more heavily 2,5'-substituted adenosine derivative, which was also a hA_{2A}AR agonist and hA₃AR antagonist.²⁰

We then examined the effects of several compounds in stimulation of cAMP production at the hA_{2B}AR expressed in CHO cells, compared to NECA as reference full agonist (= 100%). The most potent compound **4g** was a weak partial agonist in cyclic AMP accumulation (EC₅₀ ~10 μ M).¹¹ As indicated by the percent stimulation at a 10 μ M, none of other potent truncated derivatives (4'-oxo: **4a**- $1.9 \pm 4.0\%$, **4l**- $1.8 \pm 4.9\%$; 4'-thio: **4m**- $3.6 \pm 2.9\%$, **4o**- $7.0 \pm 4.4\%$) displayed significant activity at this AR subtype.

Before examining the pharmacological effect of the most potent compound **4g**, the partition coefficient (logP) was first calculated using Tripos SYBYL X-1.2 for the druggability of **4g**. LogP of **4g** was 0.51, which is sufficient to penetrate cell membranes, suggesting the possibility of bioavailability by oral as well as other administration routes.

Acute inflammation is a short-term process that is characterized by the typical signs of inflammation, such as swelling, pain, and loss of function due to the infiltration of the tissues by plasma and leukocytes. Among them, edema is one of the fundamental actions of acute inflammation and it is an essential parameter to be considered when evaluating compounds with a potential anti-inflammatory activity.²¹ Therefore, we tested the anti-inflammatory activity of **4g** on carrageenan-induced paw edema model in rats.²² Paw edema was induced by the injection of carrageenan (0.1 mL in 1% solution), and the volume of paw edema was monitored for 24 h. The paw edema was increased and reached its maximum at 4 h after treatment of carrageenan.

As shown in Figure 4, the treatment of **4g** significantly ($P < 0.01$) reduced the paw edema formation. The inhibition rate at 4 h was 51.1% with the treatment of **4g** (20 mg/kg). In the same experimental condition, indomethacin (20 mg/kg) was shown as 49.7% inhibition at 4 h.

The potency of the anti-inflammatory effect of **4g** was similar to that of indomethacin. In this study, the formation of edema reached a maximum at 4 h after carrageenan injection and the administration of **4g** inhibited the paw edema induced by carrageenan (Figure 4). These

findings demonstrated that **4g** has a potent *in vivo* anti-inflammatory activity in an acute inflammation model system.

Molecular docking study

The truncated C2-substituted derivative **4g** showed the excellent binding affinity at the hA_{2A}AR with a K_i of 7.19 nM. Substituting the N⁶ position with a chlorobenzyl group, however, dramatically decreased the hA_{2A}AR binding affinity of **4i** by 520-fold in comparison to **4g**. Our flexible docking study showed that **4g** binds readily into the antagonist-bound X-ray crystal structure of human A_{2A} AR (PDB code: 3EML)²³ (Figure 5A).¹¹ Its adenine and sugar moieties make tight interactions with the binding site residues via the π-π stacking with Phe168 and H-bonding with Glu169, Asn253 and Ser277. The C2-hexynyl group also contributes to the ligand binding through favorable hydrophobic interactions. In contrast, the N⁶-chlorobenzyl derivative **4i** appeared to have various binding modes and did not maintain some key interactions for binding (Figure 5B). It seems that **4i** would lose important interactions at the binding site in order to accommodate both the bulky N⁶-chlorobenzyl and C2-hexynyl groups. This result could explain why appending a halobenzyl group at the N⁶ position decreased the A_{2A}AR binding affinity. Furthermore, the binding modes of a series of the C2-substituted and N⁶-unsubstituted derivatives (i.e. **4a**, **4f**, **4g**, **4l**, and **4m**) were compared.

As shown in Figure 6A, the adenine and sugar moieties in this series of truncated nucleosides maintained almost exactly the same binding interactions. This docking study demonstrated that the different binding modes of the C2-substituents directly influenced their activities and a good correlation ($r^2 = 0.86$) was shown between the binding affinities and docking scores (Figure 6B). The activity of the compounds decreased as the flexibility of their C2-substituents increased. Containing the most flexible hexanyl group at the C2 position, **4f** showed a relatively low binding affinity and docking score. Taken altogether, the appropriate size of the functional group at the N⁶ position and rigidity of the C2-substituents appear to contribute to the ligand binding.

Conclusions

In summary, the series of truncated N⁶-substituted 4'-oxo- and 4'-thioadenosine derivatives, **4a-r** with substitution at C2 or C8 position, were synthesized in order to examine the structure activity relationships of this class of nucleosides as dual acting A_{2A} and A₃AR ligands. The corresponding 4'-thio- and 4'-oxonucleosides were prepared starting from D-mannose and D-erythronic γ-lactone, respectively. The highlight of our synthetic endeavor is the functionalization at the C2 position of 6-chloropurine nucleosides using lithiation-mediated stannyl transfer and palladium-catalyzed cross coupling reactions. From the study, it was revealed that an unsubstituted amino group at the N⁶ position and a hydrophobic substituent at the C2 position were required for high binding affinity at the hA_{2A}AR, but hydrophobic substitution at the C8 position abolished binding affinity at the hA_{2A}AR. However, most of the synthesized compounds displayed medium to high binding affinity at the hA₃AR, regardless of the C2- or C8-substitution. Additionally, it was also found that the geometry of the C2-substituent is crucial for the binding affinity in order of hexynyl > hexenyl > hexanyl. From this study, compounds **4g** and **4m** were discovered as a preferred ligand to act dually at the hA_{2A}AR and hA₃AR with high affinity. This mixed activity as A_{2A}AR agonist/A₃AR antagonist might be advantageous for anti-asthmatic activity. Moreover, these findings may facilitate the discrimination of the modes of binding of nucleoside derivatives at all subtypes of ARs.

Experimental Section

General methods

¹H-NMR Spectra (CDCl₃, CD₃OD or DMSO-*d*₆) were recorded on Varian Unity Inova 400 MHz. The ¹H-NMR data are reported as peak multiplicities: s for singlet, d for doublet, dd for doublet of doublets, t for triplet, q for quartet, br s for broad singlet and m for multiplet. Coupling constants are reported in hertz. ¹³C-NMR spectra (CDCl₃, CD₃OD or DMSO-*d*₆) were recorded on Varian Unity Inova 100 MHz. ¹⁹F-NMR spectra (CDCl₃, CD₃OD) were recorded on Varian Unity Inova 376 MHz. The chemical shifts were reported as parts per million (δ) relative to the solvent peak. Optical rotations were determined on Jasco III in appropriate solvent. UV spectra were recorded on U-3000 made by Hitachi in methanol or water. Infrared spectra were recorded on FT-IR (FTS-135) made by Bio-Rad. Melting points were measured on B-540 made by Buchi. Elemental analyses (C, H, and N) were used for to determine purity of all synthesized compounds, and the results were within ± 0.4% of the calculated values, confirming ≥ 95% purity. Reactions were checked with TLC (Merck precoated 60F₂₅₄ plates). Spots were detected by viewing under a UV light, coloring with charring after dipping in anisaldehyde solution with acetic acid, sulfuric acid and methanol. Column chromatography was performed on silica gel 60 (230–400 mesh, Merck). Reagents were purchased from Aldrich Chemical Company. Solvents were obtained from local suppliers. All the anhydrous solvents were distilled over CaH₂, P₂O₅ or sodium/benzophenone prior to the reaction.

Synthesis

(–)-6-Chloro-9-((3*aS*,6*R*,6*aS*)-tetrahydro-2,2-dimethylfuro[3,4-*d*][1,3]dioxol-6-yl)-9*H*-purine (6)—6-Chloropurine (0.618 g, 4.00 mmol), ammonium sulfate (0.079 g, 0.60 mmol), and hexamethyldisilazane (HMDS) (15 mL) were refluxed for 15 h under dry and inert conditions. The volatile was evaporated under high vacuum and the resulting solid was dissolved in 1,2-dichloroethane (10 mL) and cooled at 0 °C. To this solution, a solution of **5**⁹ (0.404 g, 2.00 mmol) in 1,2-dichloroethane (10 mL) and TMSOTf (0.72 mL, 4.00 mmol) were added dropwise, and the reaction mixture was stirred at 0 °C for 30 min, at room temperature for 1 h, and finally heated at 80 °C for 5 h. The mixture was cooled and diluted with CH₂Cl₂. The organic layer was washed with saturated NaHCO₃ solution, dried over anhydrous MgSO₄, and filtered. The solvent was evaporated under reduced pressure. The crude syrup was subjected to flash silica gel column chromatography (hexane : EtOAc = 2 : 1) to give **6** (0.420 g, 71%) as a white solid: mp 118–119 °C; UV (MeOH) λ_{max} 264 nm; ¹H NMR (CDCl₃) δ 8.73 (s, 1 H), 8.18 (s, 1 H), 6.10 (s, 1 H), 5.49 (d, 1 H, *J* = 6.0 Hz), 5.27–5.29 (m, 1 H), 4.25–4.31 (m, 2 H), 1.58 (s, 3 H), 1.41 (s, 3 H); ¹³C NMR (CDCl₃) δ 152.3, 151.8, 151.4, 145.1, 132.5, 113.7, 92.2, 84.7, 81.5, 76.3, 26.6, 25.0; [α]_D²⁵ –50.69 (c 0.80, MeOH); (ESI+) (M+H⁺) *m/z* 297.0752; Anal. calcd for C₁₂H₁₃ClN₄O₃: C, 48.58; H, 4.42; N, 18.88. Found: C, 48.59; H, 4.12; N, 18.08.

(–)-2-(Tributylstannyl)-6-chloro-9-((3*aS*,6*R*,6*aS*)-tetrahydro-2,2-dimethylfuro[3,4-*d*][1,3]dioxol-6-yl)-9*H*-purine (7)—To a stirred solution of 2,2,6,6-tetramethylpiperidine (TMP, 10.7 mL, 63.53 mmol) in dry hexane (15 mL) and dry THF (30 mL) was added *n*-butyllithium (41.6 mL, 1.5 M solution in hexanes, 66.7 mmol) dropwise at –78 °C over 30 min, and the mixture was stirred at the same temperature for 1 h. To this mixture, a solution of **6** (3.77 g, 12.7 mmol) in dry THF (30 mL) was added dropwise, and the mixture was stirred at –78 °C for 30 min. *n*-Tributyltin chloride (17.23 mL, 63.53 mmol) was added dropwise to the dark reaction mixture and the mixture was stirred at the same temperature for 1 h. The resulting dark solution was quenched by dropwise addition of a saturated aqueous NH₄Cl solution (50 mL). After stirred at room temperature for 15 h, the mixture was diluted with CH₂Cl₂ (100 mL). The organic layer was washed with saturated

NaHCO₃ solution, dried over anhydrous MgSO₄, and filtered. The solvent was evaporated under reduced pressure. The crude syrup was subjected to flash silica gel column chromatography (hexane : EtOAc = 5 : 1) to give **7** (7.10 g, 95%) as a colorless syrup: UV (MeOH) λ_{\max} 269 nm; ¹H NMR (CDCl₃) δ 8.06 (s, 1 H), 6.06 (s, 1 H), 5.58 (d, 1 H, *J* = 6.0 Hz), 5.30–5.32 (m, 1 H), 4.24–4.30 (m, 2 H), 1.55–1.66 (m, 9 H), 1.41 (s, 3 H), 1.27–1.38 (m, 7 H), 1.19–1.23 (m, 5 H), 0.86–0.92 (m, 9 H); ¹³C NMR (CDCl₃) δ 182.4, 150.6, 150.1, 144.1, 131.1, 113.5, 91.9, 84.6, 81.9, 76.3, 29.3, 29.2, 29.1, 27.8, 27.5, 27.2, 26.6, 24.9, 13.9, 12.7, 12.6, 10.9, 9.3, 9.2; [α]_D²⁵ –8.18 (*c* 0.33, MeOH); (ESI+) (M+H⁺) *m/z* 587.1804; Anal. calcd for C₂₄H₃₉ClN₄O₃Sn: C, 49.21; H, 6.71; N, 9.56. Found: C, 49.03; H, 6.66; N, 9.16.

(–)-6-Chloro-9-((3a*S*,6*R*,6a*S*)-tetrahydro-2,2-dimethylfuro[3,4-*d*][1,3]dioxol-6-yl)-2-iodo-9*H*-purine (8**)**—To a stirred solution of **7** (7.10 g, 12.1 mmol) in dry THF (100 mL) was added iodine (4.60 g, 18.2 mmol), and the reaction mixture was stirred for 24 h under a nitrogen atmosphere. The mixture was diluted with saturated sodium metabisulfite, stirred for 1 h, and then extracted with CH₂Cl₂ (3 × 30 mL). The organic layer was dried over anhydrous MgSO₄ and filtered. The solvent was evaporated under reduced pressure. The crude syrup was subjected to flash silica gel column chromatography (hexane : EtOAc = 3 : 1) to give **8** (4.30 g, 84%) as a white foam: UV (CH₂Cl₂) λ_{\max} 282.5 nm; ¹H NMR (CDCl₃) δ 8.07 (s, 1 H), 6.05 (s, 1 H), 5.40 (d, 1 H, *J* = 6.0 Hz), 5.25–5.28 (m, 1 H), 4.27–4.28 (m, 2 H), 1.57 (s, 3 H), 1.42 (s, 3 H); ¹³C NMR (CDCl₃) δ 152.1, 151.3, 145.1, 132.4, 116.8, 113.8, 92.1, 84.7, 81.5, 76.8, 26.6, 25.1; [α]_D²⁵ –21.88 (*c* 0.16, MeOH); (ESI+) (M+H⁺) *m/z* 422.9715; Anal. calcd for C₁₂H₁₂ClN₄O₃: C, 34.10; H, 2.86; N, 13.26. Found: C, 33.98; H, 2.77; N, 13.00.

(–)-(2*R*,3*S*,4*S*)-2-(6-Chloro-2-(hex-1-ynyl)-9*H*-purin-9-yl)-tetrahydrofuran-3,4-diol (9**)**—To a solution of **8** (1.00 g, 2.37 mmol) in anhydrous DMF (20 mL) were added tetrakis(triphenylphosphine)palladium (0.68 g, 0.59 mmol), copper iodide (0.054 g, 0.28 mmol), cesium carbonate (0.77 g, 2.37 mmol), and 1-hexyne (0.3 mL, 2.61 mmol) at room temperature, and the reaction mixture was stirred at room temperature for 3 h. The reaction mixture was evaporated and the crude product was used in the next step without further purification. To a stirred ice-cooled solution of above crude product in THF (5 mL) was added 1 *N* HCl (5 mL) and the mixture was stirred at room temperature for 15 h, neutralized with 1 *N* NaOH solution, and then evaporated under reduced pressure. The mixture was subjected to flash silica gel column chromatography (CH₂Cl₂ : MeOH = 30 : 1) to give **9** (0.42 g, 52%) as a white solid: mp 135–137 °C; UV (MeOH) λ_{\max} 281.0 nm; ¹H NMR (CD₃OD) δ 8.70 (s, 1 H), 6.05 (d, 1 H, *J* = 6.4 Hz), 4.90–4.92 (m, 1 H), 4.55 (dd, 1 H, *J* = 4.0, 9.6 Hz), 4.43–4.45 (m, 1 H), 4.02 (dd, 1 H, *J* = 1.6, 9.6 Hz), 2.50 (t, 2 H, *J* = 7.2 Hz), 1.61–1.69 (m, 2 H), 1.50–1.58 (m, 2 H), 0.98 (t, 3 H, *J* = 7.2 Hz); ¹³C NMR (CD₃OD) δ 153.1, 151.1, 147.9, 147.2, 132.1, 91.5, 91.1, 80.5, 76.6, 75.7, 72.3, 31.4, 23.1, 19.5, 13.9; [α]_D²⁵ –65.83 (*c* 0.12, MeOH); (ESI+) (M+H⁺) *m/z* 337.1062; Anal. calcd for C₁₅H₁₇ClN₄O₃: C, 53.50; H, 5.09; N, 16.64. Found: C, 53.56; H, 5.01; N, 16.34.

(–)-6-Chloro-9-((3a*S*,4*R*,6a*R*)-2,2-dimethyltetrahydrothieno[3,4-*d*][1,3]dioxol-4-yl)-2-iodo-9*H*-purine (11**)**—To a stirred solution of 2-iodo-6-chloropurine (1.90 g, 6.88 mmol) in dry CH₃CN (30 mL) was added *N,O*-bis(trimethylsilyl)acetamide (BSA, 2.24 mL, 9.16 mmol) under dry and inert conditions, and the reaction mixture was stirred at 40 °C for 45 min to obtain a clear solution. To this solution, a solution of **10**⁹ (1.00 g, 4.58 mmol) in dry CH₃CN (5 mL) was added dropwise, followed by the addition of TMSOTf (0.91 mL) at room temperature, and the mixture was heated to 80 °C for 3 h. The reaction was cooled to room temperature, quenched with saturated NaHCO₃ solution (40 mL), and diluted with EtOAc (50 mL) and then organic layers were separated. The aqueous layer was again

extracted with EtOAc (3 × 30 mL). The combined organic layers were dried over anhydrous MgSO₄, and filtered. The solvent was evaporated under reduced pressure. The residue was subjected to flash silica gel column chromatography (hexane : EtOAc = 3 : 1) to give compound **11** as a white foam (1.20 g, 60%): UV (CH₂Cl₂) λ_{max} 282.0 nm; ¹H NMR (CDCl₃) δ 8.06 (s, 1 H), 5.84 (s, 1 H), 5.33 (t, 1 H, *J* = 4.8 Hz), 5.21 (d, 1 H, *J* = 5.6 Hz), 3.80 (dd, 1 H, *J* = 4.4, 12.8 Hz), 3.25 (d, 1 H, *J* = 12.8 Hz), 1.59 (s, 3 H), 1.37 (s, 3 H); ¹³C NMR (CDCl₃) δ 151.9, 151.2, 144.4, 132.7, 116.7, 112.1, 90.0, 84.8, 70.7, 41.5, 26.6, 24.8; [α]_D²⁵ −66.33 (c 0.10, CH₂Cl₂); (ESI+) (M+H⁺) *m/z* 438.9486; Anal. calcd for C₁₂H₁₂ClIN₄O₂S: C, 32.86; H, 2.76; N, 12.77; S, 7.31. Found: C, 32.89; H, 2.89; N, 12.47; S, 7.01.

(−)-6-Chloro-9-((3*a*S,4*R*,6*a*R)-2,2-dimethyltetrahydrothieno[3,4-*d*][1,3]dioxol-4-yl)-2-(hex-1-ynyl)-9*H*-purine (12)—Compound **11** (0.60 g, 1.37 mmol) was converted to **12** (0.46 g, 86%) as a thick syrupy liquid, using the same Sonogashira conditions used in the preparation of **9**: UV (MeOH) λ_{max} 285.0 nm; ¹H NMR (CDCl₃) δ 8.16 (s, 1 H), 5.90 (s, 1 H), 5.32 (t, 1 H, *J* = 4.8 Hz), 5.21 (d, 1 H, *J* = 5.2 Hz), 3.79 (dd, 1 H, *J* = 4.4, 12.8 Hz), 3.23 (d, 1 H, *J* = 12.8 Hz), 2.48 (t, 2 H, *J* = 7.2 Hz), 1.61–1.70 (m, 2 H), 1.58 (s, 3 H), 1.47–1.54 (m, 2 H), 1.35 (s, 3 H), 0.95 (t, 3 H, *J* = 7.2 Hz); ¹³C NMR (CDCl₃) δ 151.3, 151.2, 146.3, 144.7, 130.8, 112.1, 91.3, 89.9, 843.7, 79.7, 70.2, 41.2, 30.3, 26.6, 24.8, 22.3, 19.3, 13.8; [α]_D²⁵ −57.35 (c 0.469, MeOH); (ESI+) (M+H⁺) *m/z* 393.1145; Anal. calcd for C₁₈H₂₁ClN₄O₂S: C, 55.02; H, 5.39; N, 14.26; S, 8.16. Found: C, 55.41; H, 5.21; N, 14.47; S, 8.11.

(−)-(2*R*,3*S*,4*R*)-2-(6-Chloro-2-(hex-1-ynyl)-9*H*-purin-9-yl)tetrahydrothiophene-3,4-diol (13)—Compound **12** (0.92 g, 2.34 mmol) was converted to **13** (0.58 g, 70%) as a white solid, using the same hydrolysis conditions used in the preparation of **9**: mp 76–78 °C; UV (MeOH) λ_{max} 284.5 nm; ¹H NMR (CD₃OD) δ 8.87 (s, 1 H), 6.11 (d, 1 H, *J* = 6.4 Hz), 4.69 (dd, 1 H, *J* = 3.2, 6.4 Hz), 4.48 (dd, 1 H, *J* = 3.6, 7.6 Hz), 3.56 (dd, 1 H, *J* = 4.4, 10.8 Hz), 2.97 (dd, 1 H, *J* = 3.6, 10.8 Hz), 2.51 (t, 2 H, *J* = 6.8 Hz), 1.61–1.67 (m, 2 H), 1.50–1.56 (m, 2 H), 0.98 (t, 3 H, *J* = 7.2 Hz); ¹³C NMR (CD₃OD) δ 153.6, 151.0, 148.0, 147.1, 131.9, 91.5, 80.9, 80.5, 74.4, 64.6, 35.5, 31.4, 23.1, 19.5, 14.0; [α]_D²⁵ −32.49 (c 0.634, MeOH); (ESI+) (M+H⁺) *m/z* 353.0835; Anal. calcd for C₁₅H₁₇ClN₄O₂S: C, 51.06; H, 4.86; N, 15.88; S, 9.09. Found: C, 51.09; H, 4.89; N, 15.47; S, 9.21.

(−)-9-((3*a*S,6*R*,6*a*S)-Tetrahydro-2,2-dimethylfuro[3,4-*d*][1,3]dioxol-6-yl)-2-iodo-9*H*-purin-6-amine (14)—A solution of **8** (0.303 g, 0.72 mmol) in methanolic ammonia (5 mL) was stirred for 2 h at 80 °C. The reaction mixture was evaporated and the crude residue was subjected to flash silica gel column chromatography (hexane : EtOAc = 1 : 1) to give **15** (0.205 g, 71%) as a colorless syrup: UV (CH₂Cl₂) λ_{max} 262.0 nm; ¹H NMR (DMSO-*d*₆) δ 8.16 (s, 1 H), 7.74 (br s, 2 H, D₂O exchangeable), 6.11 (s, 1 H), 5.27 (d, 1 H, *J* = 5.6 Hz), 5.13–5.15 (m, 1 H), 4.06–4.12 (m, 2 H), 1.47 (s, 3 H), 1.33 (s, 3 H); ¹³C NMR (DMSO-*d*₆) δ 155.9, 149.3, 139.8, 120.9, 118.9, 112.0, 89.2, 84.0, 80.7, 74.5, 26.2, 24.6; [α]_D²⁵ −13.25 (c 0.08, CH₂Cl₂); (ESI+) (M+H⁺) *m/z* 404.0225; Anal. calcd for C₁₂H₁₄IN₅O₃: C, 35.75; H, 3.50; N, 17.37. Found: C, 35.89; H, 3.89; N, 17.47.

(−)-9-((3*a*S,4*R*,6*a*R)-Tetrahydro-2,2-dimethylthieno[3,4-*d*][1,3]dioxol-4-yl)-2-iodo-9*H*-purin-6-amine (15)—Compound **11** (0.535 g, 1.22 mmol) was converted to **15** (0.439 g, 85%) as a colorless syrup, according to the same procedure used in the preparation of **14**: UV (CH₂Cl₂) λ_{max} 267.0 nm; ¹H NMR (CD₃OD) δ 8.20 (s, 1 H), 5.97 (s, 1 H), 5.30 (pseudo t, 1 H, *J* = 5.2 Hz), 5.23 (d, 1 H, *J* = 5.6 Hz), 3.80 (dd, 1 H, *J* = 4.4, 12.8 Hz), 3.14 (d, 1 H, *J* = 12.8 Hz), 1.54 (s, 3 H), 1.35 (s, 3 H); ¹³C NMR (CD₃OD) δ 156.1, 150.4, 141.9,

120.0, 118.0, 112.7, 91.2, 86.4, 71.3, 41.6, 26.8, 24.9; $[\alpha]^{25}_{\text{D}} -61.90$ (*c* 0.08, CH₂Cl₂); (ESI+) (M+H⁺) *m/z* 419.998; Anal. calcd for C₁₂H₁₄IN₅O₂S: C, 34.38; H, 3.37; N, 16.70; O, 7.63; S, 7.65. Found: C, 34.11; H, 3.22; N, 16.40; S, 7.45.

(-)-9-((3a*S*,6*R*,6a*S*)-Tetrahydro-2,2-dimethylfuro[3,4-*d*][1,3]dioxol-6-yl)-9*H*-purin-6-amine (18)—A solution of **6** (0.37 g, 1.25 mmol) in methanolic ammonia (5 mL) was heated for 2 h at 80 °C. The reaction mixture was evaporated and the crude residue was subjected to flash silica gel column chromatography (hexane : EtOAc = 1 : 1) to give **18** (0.27 g, 78%) as a white foam: UV (CH₂Cl₂) λ_{max} 255 nm; ¹H NMR (CDCl₃) δ 8.32 (s, 1 H), 7.89 (s, 1 H), 6.19 (brs, 2 H), 6.03 (s, 1 H), 5.48 (d, 1 H, *J* = 6.0 Hz), 5.27 (dd, 1 H, *J* = 3.2, 5.6 Hz), 4.24–4.31 (m, 2 H), 1.58 (s, 3 H), 1.41 (s, 3 H); ¹³C NMR (CDCl₃) δ 154.7, 151.3, 149.5, 141.1, 120.3, 113.5, 91.9, 84.8, 81.7, 76.1, 26.6, 25.1; $[\alpha]^{25}_{\text{D}} -35.48$ (*c* 0.09, CH₂Cl₂); (ESI+) (M+H⁺) *m/z* 278.1257; Anal. calcd for C₁₂H₁₅N₅O₃: C, 51.98; H, 5.45; N, 25.26. Found: C, 51.98; H, 5.87; N, 25.47.

(-)-8-Bromo-9-((3a*S*,6*R*,6a*S*)-tetrahydro-2,2-dimethylfuro[3,4-*d*][1,3]dioxol-6-yl)-9*H*-purin-6-amine (19)—To a solution of **18** (89 mg, 0.32 mmol) in MeOH (10 mL) and 1 *N* sodium acetate (1.7 mL) was added bromine (0.033 mL, 0.64 mmol), and the mixture was stirred at room temperature for 40 min. The mixture was diluted with saturated sodium metabisulfite solution and stirred until the red color disappeared. The volatile was evaporated and the resulting aqueous layer was extracted with EtOAc (3 × 30 mL). The combined organic layers were washed with water, dried over anhydrous MgSO₄, and filtered. The solvent was evaporated to give a pale yellowish residue. The residue was purified by flash silica gel column chromatography (hexane : EtOAc = 2 : 1) to give **19** (63 mg, 55%) as a white foam: UV (CH₂Cl₂) λ_{max} 262 nm; ¹H NMR (CDCl₃) δ 8.26 (s, 1 H), 6.20 (brs, 2 H), 6.16 (s, 1 H), 5.61 (d, 1 H, *J* = 5.6 Hz), 5.36–5.38 (m, 1 H), 4.20–4.21 (m, 2 H), 1.59 (s, 3 H), 1.42 (s, 3 H); ¹³C NMR (CDCl₃) δ 153.8, 151.9, 150.9, 128.8, 120.0, 113.2, 92.4, 84.3, 82.2, 76.5, 26.6, 24.9; $[\alpha]^{25}_{\text{D}} -28.08$ (*c* 0.26, CH₂Cl₂); (ESI+) (M+H⁺) *m/z* 356.0365; Anal. calcd for C₁₂H₁₄BrN₅O₃: C, 40.47; H, 3.96; N, 19.66. Found: C, 40.12; H, 3.88; N, 19.48.

(-)-8-Bromo-9-((3a*R*,6*R*,6a*S*)-tetrahydro-2,2-dimethylthieno[3,4-*d*][1,3]dioxol-6-yl)-9*H*-purin-2-amine (20)—8-Bromoadenine (0.40 g, 1.84 mmol) and **10** (0.20 g, 0.92 mmol) were condensed to give **20** (69 mg, 20%) as colorless syrup, according to similar procedure used in the preparation of **6**: UV (MeOH) λ_{max} 263.5 nm; ¹H NMR (CDCl₃) δ 8.25 (s, 1 H), 5.91 (s, 1 H), 5.81 (brs, 2 H, NH₂), 5.54 (d, 1 H, *J* = 5.2 Hz), 5.50 (pseudo t, 1 H, *J* = 5.2 Hz), 3.87 (dd, 1 H, *J* = 4.0, 12.4 Hz), 3.14 (d, 1 H, *J* = 12.4 Hz), 1.60 (s, 3 H), 1.38 (s, 3 H); ¹³C NMR (CDCl₃) δ 154.3, 153.0, 150.7, 127.8, 120.4, 111.4, 89.0, 86.0, 71.9, 41.4, 26.6, 24.7; $[\alpha]^{25}_{\text{D}} -77.07$ (*c* 0.16, CH₂Cl₂); (ESI+) (M+H⁺) *m/z* 373.0151; Anal. calcd for C₁₂H₁₄BrN₅O₂S: C, 38.72; H, 3.79; N, 18.81; S, 8.61. Found: C, 38.88; H, 3.88; N, 18.48; S, 8.41.

(-)-(2*R*,3*S*,4*S*)-2-(6-Amino-2-(hex-1-ynyl)-9*H*-purine-9-yl)-tetrahydrofuran-3,4-diol (4a)—A solution of **9** (0.125 g, 0.42 mmol) in NH₃/^tBuOH (5 mL) was stirred at 100 °C for 8 h. The reaction mixture was evaporated and the residue was subjected to flash silica gel column chromatography (CH₂Cl₂ : MeOH = 20 : 1) to give **4a** (0.103 g, 87%) as a white solid: mp 164–166 °C; UV (MeOH) λ_{max} 269.5 nm; ¹H NMR (CD₃OD) δ 8.26 (s, 1 H), 5.94 (d, 1 H, *J* = 6.4 Hz), 4.86–4.87 (m, 1H), 4.51 (dd, 1 H, *J* = 4.0, 9.6 Hz), 4.40–4.42 (m, 1 H), 3.98 (dd, 1 H, *J* = 2.0, 9.6 Hz), 2.45 (t, 2 H, *J* = 7.2 Hz), 1.61–1.65 (m, 2 H), 1.49–1.55 (m, 2 H), 0.98 (t, 3 H, *J* = 7.6 Hz); ¹³C NMR (CD₃OD) δ 157.2, 151.1, 148.1, 142.3, 120.1, 99.4, 88.4, 81.4, 76.6, 75.4, 72.3, 31.7, 23.2, 19.6, 14.1; $[\alpha]^{25}_{\text{D}} -39.50$ (*c* 0.16, MeOH); (ESI+)

(M+H⁺) *m/z* 318.1557; Anal. calcd for C₁₅H₁₉N₅O₃: C, 56.77; H, 6.03; N, 22.07. Found: C, 56.98; H, 5.88; N, 22.01.

General procedure for the synthesis of 4b–4e

To a solution of diol **9** in EtOH (5 mL) were added Et₃N (3 equiv) and 3-halobenzylamine (1.5 equiv) at room temperature, and the mixture was stirred at room temperature for 24 to 48 h. The solvent was evaporated and the residue was purified by a flash silica gel column chromatography (CH₂Cl₂ : MeOH = 20 : 1) to give **4b–4e** as white solids.

(–)-(2*R*,3*S*,4*S*)-2-(6-(3-Fluorobenzylamino)-2-(hex-1-ynyl)-9*H*-purin-9-yl)-tetrahydrofuran-3,4-diol (4b)—Yield: 78%; mp 206–207 °C; UV (MeOH) λ_{max} 272.0 nm; ¹H NMR (DMSO-*d*₆) δ 8.47 (brs, 1 H, D₂O exchangeable), 8.44 (s, 1 H), 7.32–7.37 (m, 1 H), 7.12–7.17 (m, 2 H), 7.02–7.07 (m, 1 H), 5.85 (d, 1 H, *J* = 6.8 Hz), 5.45 (d, 1 H, *J* = 6.4 Hz, D₂O exchangeable), 5.20 (d, 1 H, *J* = 4.0 Hz, D₂O exchangeable), 4.69–4.75 (m, 3 H), 4.33 (dd, 1 H, *J* = 3.6, 9.2 Hz), 4.24–4.25 (m, 1 H), 3.79 (dd, 1 H, *J* = 1.6, 9.2 Hz); 2.41 (t, 2 H, *J* = 7.2 Hz), 1.49–1.56 (m, 2 H), 1.38–1.47 (m, 2 H), 0.91 (t, 3 H, *J* = 7.2 Hz); ¹³C NMR (DMSO-*d*₆) δ 163.4, 161.0, 154.0, 149.1, 145.8, 142.9, 140.6, 130.2 (d), 123.1, 119.0, 113.6 (q), 87.1, 85.6, 81.6, 74.4, 73.5, 70.2, 42.4, 29.8, 21.5, 17.9, 13.4; [α]_D²⁵ –58.87 (*c* 0.23, MeOH); (ESI+) (M+H⁺) *m/z* 426.1948; Anal. calcd for C₂₂H₂₄FN₅O₃: C, 62.11; H, 5.69; N, 16.46. Found: C, 61.98; H, 5.89; N, 16.23.

(–)-(2*R*,3*S*,4*S*)-2-(6-(3-Chlorobenzylamino)-2-(hex-1-ynyl)-9*H*-purin-9-yl)-tetrahydrofuran-3,4-diol (4c)—Yield: 78%; mp 210–212 °C; UV (MeOH) λ_{max} 271.5 nm; ¹H NMR (DMSO-*d*₆) δ 8.47 (brs, 1 H, D₂O exchangeable), 8.44 (s, 1 H), 7.27–7.39 (m, 4 H), 5.84 (d, 1 H, *J* = 6.8 Hz), 5.45 (d, 1 H, *J* = 6.4 Hz, D₂O exchangeable), 5.20 (d, 1 H, *J* = 4.0 Hz, D₂O exchangeable), 4.67–4.75 (m, 3 H), 4.33 (dd, 1 H, *J* = 3.6, 9.2 Hz), 4.24–4.25 (m, 1 H), 3.79 (dd, 1 H, *J* = 1.6, 9.2 Hz); 2.41 (t, 2 H, *J* = 6.8 Hz), 1.49–1.57 (m, 2 H), 1.38–1.47 (m, 2 H), 0.91 (t, 3 H, *J* = 7.2 Hz); ¹³C NMR (DMSO-*d*₆) δ 154.0, 149.2, 145.8, 142.5, 140.6, 132.9, 130.1, 128.3, 127.0, 126.6, 125.8, 87.1, 85.7, 81.6, 74.4, 73.5, 70.2, 42.3, 29.8, 21.5, 17.9, 13.4; [α]_D²⁵ –57.46 (*c* 0.13, MeOH); (ESI+) (M+H⁺) *m/z* 442.1647; Anal. calcd for C₂₂H₂₄ClN₅O₃: C, 59.79; H, 5.47; N, 15.85. Found: C, 59.99; H, 5.55; N, 15.90.

(–)-(2*R*,3*S*,4*S*)-2-(6-(3-Bromobenzylamino)-2-(hex-1-ynyl)-9*H*-purin-9-yl)-tetrahydrofuran-3,4-diol (4d)—Yield: 73%; mp 217–218 °C; UV (MeOH) λ_{max} 273.0 nm; ¹H NMR (DMSO-*d*₆) δ 8.47 (brs, 1 H, D₂O exchangeable), 8.44 (s, 1 H), 7.54 (s, 1 H), 7.42 (d, 1 H, *J* = 7.6 Hz), 7.25–7.34 (m, 2 H), 5.84 (d, 1 H, *J* = 6.4 Hz), 5.45 (d, 1 H, *J* = 6.4 Hz, D₂O exchangeable), 5.20 (d, 1 H, *J* = 4.0 Hz, D₂O exchangeable), 4.67–4.74 (m, 3 H), 4.32 (dd, 1 H, *J* = 3.6, 9.2 Hz), 4.24–4.25 (m, 1 H), 3.79 (dd, 1 H, *J* = 1.6, 9.2 Hz); 2.41 (t, 2 H, *J* = 7.2 Hz), 1.49–1.56 (m, 2 H), 1.38–1.47 (m, 2 H), 0.91 (t, 3 H, *J* = 7.2 Hz); ¹³C NMR (DMSO-*d*₆) δ 154.0, 145.8, 142.8, 140.6, 130.5, 130.0, 129.6, 126.3, 121.5, 87.1, 85.7, 81.6, 78.8, 74.4, 73.5, 70.2, 42.3, 29.9, 21.5, 17.9, 13.4; [α]_D²⁵ –49.63 (*c* 0.14, MeOH); (ESI+) (M+H⁺) *m/z* 486.1136; Anal. calcd for C₂₂H₂₄BrN₅O₃: C, 54.33; H, 4.97; N, 14.40. Found: C, 54.23; H, 5.01; N, 14.21.

(–)-(2*R*,3*S*,4*S*)-2-(6-(3-Iodobenzylamino)-2-(hex-1-ynyl)-9*H*-purin-9-yl)-tetrahydrofuran-3,4-diol (4e)—Yield: 85%; mp 224–226 °C; UV (MeOH) λ_{max} 273.0 nm; ¹H NMR (DMSO-*d*₆) δ 8.47 (brs, 1 H, D₂O exchangeable), 8.43 (s, 1 H), 7.73 (pseudo t, 1 H, *J* = 1.6 Hz), 7.59 (d, 1 H, *J* = 7.6 Hz), 7.34 (d, 1 H, *J* = 8.0 Hz), 7.11 (pseudo t, 1 H, *J* = 8.0 Hz), 5.84 (d, 1 H, *J* = 6.4 Hz), 5.44 (brs, 1 H, D₂O exchangeable), 5.19 (d, 1 H, *J* = 2.8 Hz, D₂O exchangeable), 4.63–4.72 (m, 3 H), 4.33 (dd, 1 H, *J* = 3.6, 9.2 Hz), 4.25 (brs, 1 H), 3.79 (dd, 1 H, *J* = 1.6, 9.2 Hz); 2.41 (t, 2 H, *J* = 7.2 Hz), 1.50–1.57 (m, 2 H), 1.38–1.47 (m, 2 H), 0.91 (t, 3 H, *J* = 7.2 Hz); ¹³C NMR (DMSO-*d*₆) δ 153.9, 149.1, 145.8, 142.6, 140.6,

135.9, 135.4, 130.5, 126.6, 118.9, 94.7, 87.1, 85.7, 81.6, 74.4, 73.5, 70.2, 42.2, 29.8, 21.5, 17.9, 13.4; $[\alpha]_{\text{D}}^{25}$ -58.09 (*c* 0.14, MeOH); (ESI+) (M+H⁺) *m/z* 534.0998; Anal. calcd for C₂₂H₂₄N₅O₃: C, 49.54; H, 4.54; N, 13.13. Found: C, 49.14; H, 4.13; N, 13.01.

(-)-(2R,3S,4S)-2-(6-Amino-2-hexyl-9H-purine-9-yl)-tetrahydrofuran-3,4-diol (4f)

—A mixture of **4a** (22 mg, 0.069 mmol), absolute ethanol (5 mL), and 10% palladium on carbon (5 mg) was hydrogenated on a Parr apparatus at 40 psi for 15 h. The mixture was filtered and the solvent was evaporated to give a residue. The residue was subjected to flash silica gel column chromatography (CH₂Cl₂ : MeOH = 20 : 1) to give **4f** (15 mg, 68%) as a white solid; mp 105–107 °C; UV (MeOH) λ_{max} 261.5 nm; ¹H NMR (CD₃OD) δ 8.19 (s, 1 H), 5.95 (d, 1 H, *J* = 6.4 Hz), 4.93–4.96 (m, 1 H), 4.52 (dd, 1 H, *J* = 4.0, 9.6 Hz), 4.42–4.44 (m, 1 H), 3.99 (dd, 1 H, *J* = 1.6, 9.6 Hz), 2.74 (t, 2 H, *J* = 7.6 Hz), 1.74–1.80 (m, 2 H), 1.30–1.39 (m, 6 H), 0.88–0.92 (m, 3 H); ¹³C NMR (CD₃OD) δ 167.2, 157.1, 151.8, 141.5, 119.0, 90.5, 76.6, 75.5, 72.5, 40.0, 33.0, 30.3, 30.0, 23.8, 14.6; $[\alpha]_{\text{D}}^{25}$ -54.05 (*c* 0.11, MeOH); (ESI+) (M+H⁺) *m/z* 322.1883; Anal. calcd for C₁₅H₂₃N₅O₃: C, 56.06; H, 7.21; N, 21.79. Found: C, 56.44; H, 7.02; N, 21.49.

(-)-(2R,3S,4R)-2-(6-Amino-2-(hex-1-ynyl)-9H-purin-9-yl)tetrahydrothiophene-3,4-diol (4g)

—Compound **13** (0.065 g, 0.18 mmol) was converted to **4g** (0.051 g, 83%) as a white solid, using the same procedure in the preparation of **4a**: mp 234–235; UV (MeOH) λ_{max} 271.5 nm; ¹H NMR (DMSO-*d*₆) δ 8.47 (s, 1 H), 7.35 (br s, 2 H, D₂O exchangeable), 5.85 (d, 1 H, *J* = 7.2 Hz), 5.53 (d, 1 H, *J* = 6.4 Hz, D₂O exchangeable), 5.34 (d, 1 H, *J* = 4.0 Hz, D₂O exchangeable), 4.57–4.61 (m, 1 H), 4.33–4.35 (m, 1 H), 3.40 (dd, 1 H, *J* = 4.4, 10.8 Hz), 2.80 (dd, 1 H, *J* = 2.8, 10.8 Hz), 2.41 (t, 2 H, *J* = 6.8 Hz), 1.49–1.55 (m, 2 H), 1.40–1.46 (m, 2 H), 0.91 (t, 3 H, *J* = 7.2 Hz); ¹³C NMR (DMSO-*d*₆) δ 155.7, 149.9, 145.7, 140.4, 118.3, 85.4, 81.3, 78.5, 72.2, 61.1, 34.3, 29.9, 21.5, 17.9, 13.4; $[\alpha]_{\text{D}}^{25}$ -28.36 (*c* 0.20, MeOH); (ESI+) (M+H⁺) *m/z* 334.1336; Anal. calcd for C₁₅H₁₉N₅O₂S: C, 54.04; H, 5.74; N, 21.01; S, 9.62. Found: C, 54.44; H, 5.89; N, 21.21; S, 9.41.

General procedure for the synthesis of 4h–4k

To a solution of diol **13** in EtOH (20 mL) were added Et₃N (3 equiv) and 3-halobenzylamine (1.5 equiv) at room temperature, and the mixture was stirred at room temperature for 48 h. The solvent was evaporated and the residue was purified by a flash silica gel column chromatography (CH₂Cl₂ : MeOH = 20 : 1) to give **4h–4k** as white solids.

(-)-(2R,3S,4R)-2-(6-(3-Fluorobenzylamino)-2-(hex-1-ynyl)-9H-purin-9-yl)tetrahydrothiophene-3,4-diol (4h)

—Yield 79%; mp 200–202 °C; UV (MeOH) λ_{max} 274.0 nm; ¹H NMR (DMSO-*d*₆) δ 8.52 (s, 1 H), 8.45 (br s, 1 H, D₂O exchangeable), 7.32–7.37 (m, 1 H), 7.12–7.17 (m, 2 H), 7.02–7.07 (m, 1 H), 5.87 (d, 1 H, *J* = 7.2 Hz), 5.54 (d, 1 H, *J* = 6.0 Hz, D₂O exchangeable), 5.36 (d, 1 H, *J* = 4.4 Hz, D₂O exchangeable), 4.68 (br s, 2 H), 4.58–4.62 (m, 1 H), 4.34–4.35 (m, 1 H), 3.41 (dd, 1 H, *J* = 4.4, 10.8 Hz), 2.80 (dd, 1 H, *J* = 2.8, 10.8 Hz), 2.40 (t, 2 H, *J* = 7.2 Hz), 1.49–1.55 (m, 2 H), 1.39–1.47 (m, 2 H), 0.91 (t, 3 H, *J* = 7.2 Hz); ¹³C NMR (DMSO-*d*₆) δ 163.4, 160.9, 154.0, 149.4, 145.6, 143.0, 140.5, 130.2 (d), 123.1, 118.6, 113.6 (q), 85.7, 81.5, 78.6, 72.2, 61.1, 42.4, 34.4, 29.8, 21.5, 17.9, 13.4; $[\alpha]_{\text{D}}^{25}$ -48.91 (*c* 0.184, MeOH); (ESI+) (M+H⁺) *m/z* 442.1708; Anal. calcd for C₂₂H₂₄FN₅O₂S: C, 59.85; H, 5.48; N, 15.86; S, 7.26. Found: C, 59.84; H, 5.88; N, 15.47; S, 7.21.

(-)-(2R,3S,4R)-2-(6-(3-Chlorobenzylamino)-2-(hex-1-ynyl)-9H-purin-9-yl)tetrahydrothiophene-3,4-diol (4i)

—Yield 72%; mp 199–201 °C; UV (MeOH) λ_{max} 275.0 nm; ¹H NMR (DMSO-*d*₆) δ 8.52 (s, 1 H), 8.46 (br s, 1 H, D₂O exchangeable), 7.27–

7.39 (m, 4 H), 5.87 (d, 1 H, $J = 7.6$ Hz), 5.54 (d, 1 H, $J = 6.4$ Hz, D₂O exchangeable), 5.35 (d, 1 H, $J = 4.4$ Hz, D₂O exchangeable), 4.58–4.67 (m, 3 H), 4.33–4.35 (m, 1 H), 3.41 (dd, 1 H, $J = 4.0, 10.8$ Hz), 2.80 (dd, 1 H, $J = 3.2, 10.8$ Hz), 2.41 (t, 2 H, $J = 7.2$ Hz), 1.50–1.57 (m, 2 H), 1.38–1.47 (m, 2 H), 0.91 (t, 3 H, $J = 7.2$ Hz); ¹³C NMR (DMSO-*d*₆) δ 153.9, 149.4, 145.7, 142.5, 140.5, 132.9, 130.1, 127.0, 126.6, 125.8, 118.7, 85.7, 81.6, 78.6, 72.2, 61.1, 42.3, 34.4, 29.8, 21.5, 17.9, 13.4; [α]²⁵_D -46.67 (*c* 0.30, MeOH); (ESI+) (M+H⁺) *m/z* 458.1415; Anal. calcd for C₂₂H₂₄ClN₅O₂S: C, 57.70; H, 5.28; N, 15.29; S, 7.00. Found: C, 57.41; H, 5.68; N, 15.47; S, 7.00.

(-)-(2R,3S,4R)-2-(6-(3-Bromobenzylamino)-2-(hex-1-ynyl)-9H-purin-9-yl)tetrahydrothiophene-3,4-diol (4j)—Yield 81%; mp 206–208 °C; UV (MeOH) λ_{max} 275.5 nm; ¹H NMR (DMSO-*d*₆) δ 8.52 (s, 1 H), 8.46 (br s, 1 H, D₂O exchangeable), 7.54 (s, 1 H), 7.42 (d, 1 H, $J = 8.0$ Hz), 7.33 (d, 1 H, $J = 7.6$ Hz), 7.27 (t, 1 H, $J = 7.6$ Hz), 5.87 (d, 1 H, $J = 7.2$ Hz), 5.84 (d, 1 H, $J = 6.4$ Hz, D₂O exchangeable), 5.36 (d, 1 H, $J = 4.0$ Hz, D₂O exchangeable), 4.60–4.66 (m, 3 H), 4.34–4.35 (m, 1 H), 3.40 (dd, 1 H, $J = 4.0, 10.8$ Hz), 2.80 (dd, 1 H, $J = 3.2, 10.8$ Hz), 2.41 (t, 2 H, $J = 7.2$ Hz), 1.51–1.55 (m, 2 H), 1.39–1.45 (m, 2 H), 0.91 (t, 3 H, $J = 7.2$ Hz); ¹³C NMR (DMSO-*d*₆) δ 153.9, 149.4, 145.6, 142.7, 140.5, 130.4, 129.9, 129.5, 126.2, 121.5, 118.6, 85.7, 81.5, 78.6, 72.2, 61.1, 42.3, 34.4, 29.8, 21.5, 17.9, 13.4; [α]²⁵_D -52.17 (*c* 0.207, MeOH); (ESI+) (M+H⁺) *m/z* 504.0890; Anal. calcd for C₂₂H₂₄BrN₅O₂S: C, 52.59; H, 4.81; N, 13.94; S, 6.38. Found: C, 52.22; H, 4.89; N, 13.57; S, 5.99.

(-)-(2R,3S,4R)-2-(6-(3-Iodobenzylamino)-2-(hex-1-ynyl)-9H-purin-9-yl)tetrahydrothiophene-3,4-diol (4k)—Yield 77%; mp 225–227 °C; UV (MeOH) λ_{max} 274.5 nm; ¹H NMR (DMSO-*d*₆) δ 8.52 (s, 1 H), 8.45 (br s, 1 H, D₂O exchangeable), 7.73 (s, 1 H), 7.58 (d, 1 H, $J = 8.0$ Hz), 7.34 (d, 1 H, $J = 7.6$ Hz), 7.11 (t, 1 H, $J = 7.6$ Hz), 5.87 (d, 1 H, $J = 7.2$ Hz), 5.54 (d, 1 H, $J = 6.0$ Hz, D₂O exchangeable), 5.36 (d, 1 H, $J = 4.0$ Hz, D₂O exchangeable), 4.57–4.62 (m, 3 H), 4.32–4.36 (m, 1 H), 3.40 (dd, 1 H, $J = 4.0, 10.8$ Hz), 2.80 (dd, 1 H, $J = 3.2, 10.8$ Hz), 2.42 (t, 2 H, $J = 7.2$ Hz), 1.50–1.57 (m, 2 H), 1.38–1.47 (m, 2 H), 0.91 (t, 3 H, $J = 7.2$ Hz); ¹³C NMR (DMSO-*d*₆) δ 153.9, 149.4, 145.6, 142.6, 140.5, 135.9, 135.4, 130.5, 126.6, 118.6, 94.7, 85.7, 81.5, 78.6, 72.1, 61.1, 42.2, 34.3, 29.8, 21.5, 17.9, 13.4; [α]²⁵_D -43.33 (*c* 0.18, MeOH); (ESI+) (M+H⁺) *m/z* 550.0764; Anal. calcd for C₂₂H₂₄I N₅O₂S: C, 48.09; H, 4.40; N, 12.75; S, 5.84. Found: C, 48.09; H, 4.21; N, 12.47; S, 6.01.

(-)-(2R,3S,4S)-2-(6-Amino-2-((E)-hex-1-enyl)-9H-purin-9-yl)-tetrahydrofuran-3,4-diol (4l)—A mixture of **14** (0.096 g, 0.24 mmol), tetrakis(triphenylphosphine) palladium (28 mg, 0.024 mmol), sodium carbonate (76 mg, 0.72 mmol), and (*E*)-1-catecholboranylhexene (67 mg, 0.33 mmol) in DMF and H₂O (8 : 1, 5 mL) was stirred at 90 °C for 15 h. The reaction mixture was filtered over a Celite bed, and the residue was evaporated to give the crude compound **16**. To a solution of **16** in THF (5 mL) was added 1 *N* HCl (5 mL), and the mixture was stirred at room temperature for 15 h. The mixture was neutralized with 1 *N* NaOH, and then carefully evaporated under reduced pressure. The crude residue was subjected to flash silica gel column chromatography (CH₂Cl₂ : MeOH = 20 : 1) to give **4l** (48 mg, 63%) as a white solid: mp 165–167 °C; UV (MeOH) λ_{max} 293.0 nm; ¹H NMR (CD₃OD) δ 8.20 (s, 1 H), 6.99–7.06 (m, 1 H), 6.36 (tt, 1 H, $J = 1.6, 15.6$ Hz), 5.97 (d, 1 H, $J = 6.4$ Hz), 4.94 (dd, 1 H, $J = 4.8, 6.0$ Hz), 4.53 (dd, 1 H, $J = 4.0, 9.6$ Hz); 4.43–4.46 (m, 1 H), 3.99 (dd, 1 H, $J = 2.0, 9.6$ Hz), 2.25–2.31 (m, 2 H), 1.47–1.54 (m, 2 H), 1.36–1.45 (m, 2 H), 0.95 (t, 3 H, $J = 7.2$ Hz); ¹³C NMR (CD₃OD) δ 160.9, 156.9, 151.7, 141.6, 141.3, 130.7, 90.3, 76.4, 75.4, 72.4, 57.9, 33.3, 32.3, 23.4, 14.3; [α]²⁵_D -47.05 (*c* 0.12, MeOH); (ESI+) (M+H⁺) *m/z* 320.1747; [α]²⁵_D -44.80 (*c* 0.12,

MeOH); Anal. calcd for C₁₅H₂₁N₅O₃: C, 56.41; H, 6.63; N, 21.90. Found: C, 56.78; H, 6.89; N, 21.77.

(–)-(2R,3S,4R)-2-(6-Amino-2-(E)-hex-1-enyl)-9H-purine-9-yl)-tetrahydrothiophene-3,4-diol (4m)—

Compound **15** (46 mg, 0.11 mmol) was converted to **4m** (23 mg, 63%) as a white solid, according to the same procedure used in the preparation of **4l**: mp 209–210 °C; UV (MeOH) λ_{max} 274.5 nm; ¹H NMR (DMSO-*d*₆) δ 8.37 (s, 1 H), 7.11 (brs, 2 H, NH₂), 6.87–6.94 (m, 1 H), 6.29 (d, 1 H, *J* = 15.2 Hz), 5.89 (d, 1 H, *J* = 7.2 Hz), 5.52 (d, 1 H, OH, *J* = 6.0 Hz), 5.36 (d, 1 H, OH, *J* = 4.0 Hz), 4.63–4.67 (m, 1 H), 4.37 (pseudo t, 1 H, *J* = 3.2 Hz), 3.42 (dd, 1 H, *J* = 4.4, 10.8 Hz), 2.80 (dd, 1 H, *J* = 2.8, 10.8 Hz); 2.20–2.26 (m, 2 H), 1.41–1.48 (m, 2 H), 1.29–1.38 (m, 2 H), 0.90 (t, 3 H, *J* = 7.2 Hz); ¹³C NMR (DMSO-*d*₆) δ 158.2, 155.5, 150.6, 139.6, 138.2, 130.4, 117.7, 78.5, 72.3, 61.0, 34.4, 31.4, 30.5, 21.7, 13.8; [α]_D²⁵ –44.80 (*c* 0.12, MeOH); (ESI+) (M+H⁺) *m/z* 336.1499; Anal. calcd for C₁₅H₂₁N₅O₂S: C, 53.71; H, 6.31; N, 20.88; S, 9.56. Found: C, 53.89; H, 6.71; N, 20.49; S, 9.32.

(–)-(2R,3S,4S)-2-(6-Amino-8-(hex-1-ynyl)-9H-purine-9-yl)-tetrahydrofuran-3,4-diol (4n)—

Compound **19** (0.605 g, 0.19 mmol) was dissolved in Et₃N (10 mL) and DMF (10 mL). After purging the solution with N₂, (Ph₃P)₂PdCl₂ (0.238 g, 0.34 mmol), CuI (0.065 g, 0.34 mmol), and 1-hexyne (0.49 mL, 4.25 mmol) were subsequently added dropwise. The mixture was stirred at room temperature for 3 h. The volatiles were evaporated to give the crude compound **21**. To a solution of **21** in THF (10 mL) was added 1 *N* HCl (10 mL), and the mixture was stirred at room temperature for 15 h. The mixture was neutralized with 1 *N* NaOH, and then evaporated under reduced pressure. The crude residue was subjected to flash silica gel column chromatography (CH₂Cl₂ : MeOH = 10 : 1) to give **4n** (0.334 g, 62%) as a white solid: mp 228–232 °C; UV (MeOH) λ_{max} 291.5 nm; ¹H NMR (CD₃OD) δ 8.19 (s, 1 H), 6.14 (d, 1 H, *J* = 7.2 Hz), 5.32 (dd, 1 H, *J* = 4.8, 6.8 Hz), 4.57 (dd, 1 H, *J* = 3.2, 9.6 Hz), 4.43–4.45 (m, 1 H), 3.99 (dd, 1 H, *J* = 1.2, 9.6 Hz), 2.59 (t, 2 H, *J* = 6.8 Hz), 1.64–1.70 (m, 2 H), 1.52–1.58 (m, 2 H), 1.00 (t, 3 H, *J* = 7.2 Hz); ¹³C NMR (CD₃OD) δ 156.9, 154.4, 150.6, 136.7, 120.3, 99.9, 91.1, 76.1, 75.1, 72.9, 70.8, 31.2, 23.1, 19.7, 13.9; [α]_D²⁵ –42.75 (*c* 0.14, MeOH); (ESI+) (M+H⁺) *m/z* 318.1568; Anal. calcd for C₁₅H₁₉N₅O₃: C, 56.77; H, 6.03; N, 22.07. Found: C, 56.89; H, 6.23; N, 22.47.

(–)-(2R,3S,4R)-2-(6-Amino-8-(hex-1-ynyl)-9H-purine-9-yl)-tetrahydrothiophene-3,4-diol (4o)—

Compound **20** (69 mg, 0.19 mmol) was converted to **4o** (36 mg, 58%) as a white solid, according to the same procedure used in the preparation of **4n**: mp 234–235 °C; UV (MeOH) λ_{max} 294.0 nm; ¹H NMR (DMSO-*d*₆) δ 8.16 (s, 1 H), 7.40 (brs, 2 H, NH₂), 6.03 (d, 1 H, *J* = 7.6 Hz), 5.44 (d, 1 H, -OH, *J* = 6.4 Hz), 5.33 (d, 1 H, OH, *J* = 4.0 Hz), 5.24–5.29 (m, 1 H), 4.40 (dd, 1 H, *J* = 1.6, 3.2 Hz), 3.42 (dd, 1 H, *J* = 3.6, 11.2 Hz), 2.80 (dd, 1 H, *J* = 2.0, 11.2 Hz), 2.59 (t, 2 H, *J* = 6.8 Hz), 1.55–1.62 (m, 2 H), 1.44–1.51 (m, 2 H), 0.93 (t, 3 H, *J* = 7.2 Hz); ¹³C NMR (DMSO-*d*₆) δ 155.7, 153.1, 149.1, 133.7, 118.9, 98.0, 76.5, 72.3, 70.7, 63.2, 35.5, 29.6, 21.4, 18.3, 13.4; [α]_D²⁵ –112.2 (*c* 0.14, MeOH); (ESI+) (M+H⁺) *m/z* 334.1339; Anal. calcd for C₁₅H₁₉N₅O₂S: C, 54.04; H, 5.74; N, 21.01; S, 9.62. Found: C, 54.43; H, 5.88; N, 19.94; S, 9.31.

(–)-(2R,3S,4S)-2-(6-Amino-8-hexyl-9H-purine-9-yl)-tetrahydrofuran-3,4-diol (4p)

—A mixture of **4n** (0.116 g, 0.36 mmol), absolute ethanol (20 mL), and 10% palladium on carbon (20 mg) was hydrogenated on a Parr apparatus at 40 psi for 15 h. The mixture was filtered and the solvent was evaporated. The mixture was subjected to flash silica gel column chromatography (CH₂Cl₂ : MeOH = 20 : 1) to give **4p** (81 mg, 69%) as a white solid: mp 228–229 °C; UV (MeOH) λ_{max} 259.5 nm; ¹H NMR (DMSO-*d*₆) δ 8.14 (s, 1 H), 7.41 (brs, 2 H, D₂O exchangeable), 5.76 (d, 1 H, *J* = 6.8 Hz), 5.37 (brs, 1 H, D₂O exchangeable), 5.25

(brs, 1 H, D₂O exchangeable), 5.13–5.15 (m, 1 H), 4.40 (dd, 1 H, $J = 3.2, 9.2$ Hz), 4.28 (pseudo t, 1 H, $J = 3.2$ Hz), 3.83 (d, 1 H, $J = 9.2$ Hz), 2.82–2.87 (m, 2 H), 1.69–1.77 (m, 2 H), 1.32–1.39 (m, 2 H), 1.26–1.31 (m, 4 H), 0.85–0.88 (m, 3 H); ¹³C NMR (DMSO-*d*₆) δ 154.3, 152.9, 150.5, 150.1, 118.1, 88.3, 74.3, 73.2, 70.7, 30.9, 28.4, 27.6, 27.4, 22.0, 13.9; [α]²⁵_D –36.50 (*c* 0.13, MeOH); (ESI+) (M+H⁺) m/z 322.1883; Anal. calcd for C₁₅H₂₃N₅O₃: C, 56.06; H, 7.21; N, 21.79. Found: C, 56.45; H, 7.22; N, 21.77.

(–)-(2R,3S,4S)-2-(6-Amino-8-(hex-1-enyl)-9H-purine-9-yl)-tetrahydrofuran-3,4-diol (4q)—A mixture of **19** (78.8 mg, 0.22 mmol), tetrakis(triphenylphosphine) palladium(0) (26 mg, 0.022 mmol), sodium carbonate (70 mg, 0.66 mmol), and (*E*)-1-catecholboranylhexene (134 mg, 0.66 mmol) in DMF and H₂O (8 : 1, 5 mL) was stirred for 15 h at 90 °C. The reaction mixture was filtered by a bed of Celite, and the volatiles were evaporated to give the crude compound **23**. To a solution of **23** in THF (3 mL) was added 1 *N* HCl (3 mL), and the mixture stirred at room temperature for 15 h. The mixture was neutralized with 1 *N* NaOH solution, and then carefully evaporated under reduced pressure. The mixture was subjected to flash silica gel column chromatography (CH₂Cl₂ : MeOH = 20 : 1) to give **4q** (41 mg, 58%) as a white solid: mp 204–206 °C; UV (MeOH) λ_{\max} 296.5 nm; ¹H NMR (DMSO-*d*₆) δ 8.08 (s, 1 H), 7.18 (brs, 2 H, D₂O exchangeable), 6.84–6.92 (m, 1 H), 6.58 (tt, 1 H, $J = 1.6, 15.6$ Hz), 5.91 (d, 1 H, $J = 6.8$ Hz), 5.36 (d, 1 H, $J = 6.8$ Hz, D₂O exchangeable), 5.21 (d, 1 H, $J = 4.0$ Hz, D₂O exchangeable), 5.05–5.06 (m, 1 H), 4.37 (dd, 1 H, $J = 3.6, 9.6$ Hz), 4.28 (d, 1 H, $J = 3.6$ Hz), 3.82 (dd, 1 H, $J = 1.2, 9.6$ Hz); 2.28–2.34 (m, 2 H), 1.43–1.50 (m, 2 H), 1.31–1.40 (m, 2 H), 0.91 (t, 3 H, $J = 7.6$ Hz); ¹³C NMR (DMSO-*d*₆) δ 155.4, 151.9, 150.2, 148.0, 140.8, 118.8, 116.6, 87.6, 74.1, 73.3, 70.5, 32.0, 30.3, 21.7, 13.7; [α]²⁵_D –24.76 (*c* 0.11, MeOH); (ESI+) (M+H⁺) m/z 320.1717; Anal. calcd for C₁₅H₂₁N₅O₃: C, 56.41; H, 6.63; N, 21.93. Found: C, 56.32; H, 6.85; N, 21.89.

(–)-(2R,3S,4R)-2-(6-Amino-8-(hex-1-enyl)-9H-purine-9-yl)-tetrahydrothiophene-3,4-diol (4r)—Compound **20** (42 mg, 0.12 mmol) was converted to **4r** (25 mg, 65%) as a white solid, according to the same procedure used in the preparation of **4q**: mp 248–249 °C; UV (MeOH) λ_{\max} 297.5 nm; ¹H NMR (CD₃OD) δ 8.15 (s, 1 H), 6.94–7.01 (m, 1 H), 6.60 (d, 1 H, $J = 15.2$ Hz), 6.15 (d, 1 H, $J = 8.0$ Hz), 5.27 (dd, 1 H, $J = 3.6, 8.0$ Hz), 4.48–4.50 (m, 1 H), 3.65 (dd, 1 H, $J = 3.6, 11.6$ Hz), 2.93 (dd, 1 H, $J = 1.6, 11.6$ Hz), 2.36–2.42 (m, 2 H), 1.53–1.58 (m, 2 H), 1.42–1.50 (m, 2 H), 0.98 (t, 3 H, $J = 7.2$ Hz); ¹³C NMR (CD₃OD) δ 153.5, 152.9, 151.8, 151.2, 143.9, 120.1, 117.4, 78.8, 74.4, 63.9, 36.3, 32.0, 32.1, 23.4, 14.3; [α]²⁵_D –71.56 (*c* 0.10, MeOH); (ESI+) (M+H⁺) m/z 336.1494; Anal. calcd for C₁₅H₂₁N₅O₂S: C, 53.71; H, 6.31; N, 20.88; S, 9.56. Found: C, 53.56; H, 6.33; N, 20.67; S, 9.45.

Pharmacology

In vitro assays

Cell culture and membrane preparation: CHO cells stably expressing either the recombinant hA₁ or hA₃AR and HEK-293 cells stably expressing the human A_{2A}AR were cultured in Dulbecco's modified eagle's medium (DMEM) and F12 (1:1) supplemented with 10% fetal bovine serum, 100 units/mL penicillin, 100 μ g/mL streptomycin, and 2 μ mol/mL glutamine. In addition, we added 800 μ g/mL Geneticin to the hA_{2A}AR media and 500 μ g/mL Hygromycin B to the hA₁AR, hA_{2B}AR, and hA₃AR media. After harvesting the cells, we centrifuged them at 250g for 5 min at 4 °C. The pellet was resuspended in 50 mM Tris-HCl buffer (pH 7.5), containing 10 mM MgCl₂. The suspension was homogenized with an electric homogenizer for 10 s and was then recentrifuged at 20,000g for 30 min at 4 °C. The resultant pellet was homogenized again, resuspended in the buffer mentioned above in the presence of 3 U/mL adenosine deaminase, finally pipetted into 1 mL vials, and stored at

–80°C until the binding experiments were conducted. The concentration of protein was determined using a BCA Protein Assay Kit from Pierce Biotechnology (Rockford, IL).²⁴

Radioligand binding assay: Radioligand binding assays with A₁, A_{2A}, and A₃ARs were performed according to the procedures described previously.^{25–27} Briefly, for binding to human A₁ receptors, [³H]PIA (1 nM) was incubated with membranes (40 µg/tube) from CHO cells stably expressing human A₁ receptors at 25 °C for 60 min in 50 mM Tris-HCl buffer (pH 7.4; MgCl₂, 10 mM) in a total assay volume of 200 µL. Nonspecific binding was determined using 10 µM of **25**. For human A_{2A} receptor binding, membranes (20 µg/tube) from HEK-293 cells stably expressing human A_{2A}ARs were incubated with 15 nM [³H]**26** at 25 °C for 60 min in 200 µl 50 mM Tris-HCl, pH 7.4, containing 10 mM MgCl₂. Reaction was terminated by filtration with GF/B filters. For competitive binding assay to human A₃ARs, each tube contained 100 µL suspension of membranes (20 µg protein) from CHO cells stably expressing the human A₃AR, 50 µL of [¹²⁵I]**27** (0.5 nM), and 50 µL of increasing concentrations of the nucleoside derivative in Tris-HCl buffer (50 mM, pH 7.4) containing 10 mM MgCl₂, 1 mM EDTA. Nonspecific binding was determined using 10 µM of **25** in the buffer. The mixtures were incubated at 25 °C for 60 min. Binding reactions were terminated by filtration through Whatman GF/B filters under reduced pressure using a MT-24 cell harvester (Brandell, Gaithersburgh, MD, USA). Filters were washed three times with 9 mL ice-cold buffer. Radioactivity was determined in a Beckman 5500B γ-counter.

For binding at all three subtypes, K_i values are expressed as mean ± sem, n = 3–5 (outliers eliminated), and normalized against a non-specific binder, 10 µM **25**. Alternately, for weak binding a percent inhibition of specific radioligand binding at 10 µM, relative to inhibition by 10 µM **25** assigned as 100%, is given.

cAMP accumulation assay: Intracellular cAMP levels were measured with a competitive protein binding method.²⁸ CHO cells that expressed the recombinant hA_{2A}AR, hA_{2B}AR, or hA₃AR were harvested by trypsinization. After centrifugation and resuspended in medium, cells were planted in 24-well plates in 1.0 mL medium. After 24 h, the medium was removed and cells were washed three times with 1 mL DMEM, containing 50 mM HEPES, pH 7.4. Cells were then treated with the test agonist in the presence of rolipram (10 µM) and adenosine deaminase (3 units/mL). For the hA_{2A}AR and the hA_{2B}AR, incubation with agonist was performed for 30 min. For the hA₃AR, after 30 min forskolin (10 µM) was added to the medium, and incubation was continued for an additional 15 min. The reaction was terminated by removing the supernatant, and cells were lysed upon the addition of 200 µL of 0.1 M ice-cold HCl. The cell lysate was resuspended and stored at –20°C. For determination of cAMP production, 100 µl of the HCl solution was used in the Sigma Direct cAMP Enzyme Immunoassay following the instructions provided with the kit. The results were interpreted using a Bio-Tek Instruments ELx808 Ultra Microplate reader at 405 nm.

Data analysis: Binding and functional parameters were calculated using the Prism 5.0 software (GraphPAD, San Diego, CA, USA). IC₅₀ values obtained from competition curves were converted to K_i values using the Cheng-Prusoff equation.²⁹ Data were expressed as mean ± standard error.

In vivo assay of anti-inflammatory effect

Animals: Male Sprague Dawley (SD) rats (140–160 g, 5 weeks old) were purchased from Central Laboratory Animal Inc. (Seoul, Korea). Animals were housed under standard laboratory conditions with free access to food and water. The temperature was thermostatically regulated to 22 °C ± 2 °C, and a 12-hour light/dark schedule was maintained. Prior to their use, they were allowed one week for acclimatization within the

work area environment. All animal experiments were carried out in accordance with Institutional Animal Care and Use Committee Guidelines of Seoul National University (SNU-201110-4).

Carrageenan-induced paw edema: Carrageenan-induced hind paw edema model in rats was used for the assessment of anti-inflammatory activity.³⁰ Test compounds **4g** (20 mg/kg) and indomethacin (20 mg/kg) were administered by an intraperitoneal injection dissolved in 5% cremophor and 5% ethanol in PBS, and solvent alone was served as a vehicle control. Thirty minutes after the administration of **4g**, vehicle, or indomethacin, paw edema was induced by subplantar injection of 0.1 mL of 1% freshly prepared carrageenan suspension in normal saline into the right hind paw of each rat. The left hind paw was injected with 0.1 mL of normal saline. The paw volume was measured before (0 h) and at intervals of 0.5, 1, 2, 4, 6 and 24 h after carrageenan injection using a plethysmometer (Ugo Basile, Comerio, Italy).

Statistics: All experiments were repeated at least three times. Data were presented as means \pm SD for the indicated number of independently performed experiments. The statistical significances within a parameter were evaluated by one-way and multiple analysis of variation (ANOVA).

Molecular modeling—The 3D structures of the molecules were generated with Concord and energy minimized using MMFF94s force field and MMFF94 charge until the rms of Powell gradient was $0.05 \text{ kcal mol}^{-1} \text{ \AA}^{-1}$ in SYBYL-X 1.2 (Tripos International, St. Louis, MO, USA). The X-ray crystal structure of the A_{2A} AR (PDB ID: 3EML) was prepared by Biopolymer Structure Preparation Tool in SYBYL. The docking study was performed using GOLD v.5.0.1 (Cambridge Crystallographic Data Centre, Cambridge, UK), which employs a genetic algorithm (GA) and allows for full ligand flexibility and partial protein flexibility. The region of 9 Å around the co-crystallized ligand was defined as the binding site. The side chains of the eight residues (i.e., Thr88, Phe168, Glu169, Trp246, Leu249, Asn253, Ser277, and His278), which are important for ligand binding, were set to be flexible with 'crystal mode'. GoldScore scoring function was used and other parameters were set as default except the number of GA runs as 30. The Fast Connolly surface of the receptor and the van der Waals surface of each ligand were generated by MOLCAD in SYBYL. All computation calculations were undertaken on Intel® Xeon™ Quad-core 2.5 GHz workstation with Linux Cent OS release 5.5.

Supplementary Material

Refer to Web version on PubMed Central for supplementary material.

Acknowledgments

This work was supported by the grants from Basic Science Research (2008-314-E00304), the National Core Research Center (2011-0006244), the World Class University (R31-2008-000-10010-0), National Leading Research Lab Program (2011-0028885), and Brain Research Center of the 21st Century Frontier Research (2011K000289) from National Research Foundation (NRF), Korea, and the Intramural Research Program of NIDDK, NIH, Bethesda, MD, USA.

ABBREVIATIONS

AR	adenosine receptor
Cl-IB-MECA	2-chloro- <i>N</i> ⁶ -(3-iodobenzyl)-5'- <i>N</i> -methylcarbamoyladenine

Thio-Cl-IB-MECA	2-chloro- <i>N</i> ⁶ -(3-iodobenzyl)-5'- <i>N</i> -methylcarbamoyl-4'-thioadenosine
TMSOTf	trimethylsilyl trifluoromethanesulfonate
NOE	nuclear Overhauser effect
R-PIA	(-)- <i>N</i> ⁶ -2-phenylisopropyl adenosine
I-AB-MECA	<i>N</i> ⁶ -(3-iodo-4-aminobenzyl)-5'- <i>N</i> -methylcarboxamidoadenosine
NECA	5'- <i>N</i> -ethylcarboxamidoadenosine
HMDS	hexamethyldisilazane
BSA	<i>N,O</i> -bis(trimethylsilyl)acetamide
DMEM	Dulbecco's modified eagle's medium
CHO	Chinese hamster ovary
HEK	human embryonic kidney
cAMP	cyclic adenosine-5'-monophosphate

References

- Olah ME, Stiles GL. The role of receptor structure in determining adenosine receptor activity. *Pharmacol Ther.* 2000; 85:55–75. [PubMed: 10722120]
- Fredholm BB, Cunha RA, Svenningsson P. Pharmacology of adenosine receptors and therapeutic applications. *Curr Top Med Chem.* 2002; 3:413–426. [PubMed: 12570759]
- Baraldi PG, Cacciari B, Romagnoli R, Merighi S, Varani K, Borea PA, Spalluto G. A₃ adenosine receptor ligands: history and perspectives. *Med Res Rev.* 2000; 20:103–128. [PubMed: 10723024]
- Jacobson KA, Gao ZG. Adenosine receptors as therapeutic targets. *Nature Rev Drug Disc.* 2006; 5:247–264.
- Kim HO, Ji X-d, Siddiqi SM, Olah ME, Stiles GL, Jacobson KA. 2-Substitution of *N*⁶-benzyladenosine-5'-uronamides enhances selectivity for A₃ adenosine receptors. *J Med Chem.* 1994; 37:3614–3621. [PubMed: 7932588]
- (a) Jeong LS, Jin DZ, Kim HO, Shin DH, Moon HR, Gunaga P, Chun MW, Kim YC, Melman N, Gao ZG, Jacobson KA. *N*⁶-Substituted D-4'-thioadenosine-5'-methyluronamides: Potent and selective agonists at the human A₃ adenosine receptor. *J Med Chem.* 2003; 46:3775–3777. [PubMed: 12930138] (b) Jeong LS, Lee HW, Jacobson KA, Kim HO, Shin DH, Lee JA, Gao Z-G, Lu C, Duong HT, Gunaga P, Lee SK, Jin DZ, Chun MW, Moon HR. Structureactivity relationships of 2-chloro-*N*⁶-substituted-4'-thioadenosine-5'-uronamides as highly potent and selective agonists at the human A₃ adenosine receptor. *J Med Chem.* 2006; 49:273–281. [PubMed: 16392812]
- Lee EJ, Min HY, Chung HJ, Park EJ, Shin DH, Jeong LS, Lee SK. A novel adenosine analog, thio-Cl-IB-MECA, induces G₀/G₁ cell cycle arrest and apoptosis in human promyelocytic leukemia HL-60 cells. *Biochem. Pharmacol.* 2005; 70: 918–924. (b) Bar-Yehuda, S., Stemmer, S. M., Madi, L., Castel, D., Ochaion, A., Cohen, S., Barer, F., Zabutti, A., Perez-Liz, G., Del Valle, L., Fishman, P. The A₃ adenosine receptor agonist CF102 induces apoptosis of hepatocellular carcinoma via deregulation of the Wnt and NF-κB signal transduction pathways, *Int. J. Oncol.* 2008; 33: 287–295. (c) Kohno, Y., Sei, Y., Koshiba, M., Kim, H. O., Jacobson, K. A. Induction of apoptosis in HL-60 human promyelocytic leukemia cells by selective adenosine A₃ receptor agonists. *Biochem Biophys Res Comm.* 1996; 219:904–910. [PubMed: 8645277]
- Kim SK, Jacobson KA. Three-dimensional quantitative structure-activity relationship of nucleosides acting at the A₃ adenosine receptor: Analysis of binding and relative efficacy. *J Chem Inf Model.* 2007; 47:1225–1231. [PubMed: 17338510]
- Jeong LS, Choe SA, Gunaga P, Kim HO, Lee HW, Lee SK, Tosh DK, Patel A, Palaniappan KK, Gao ZG, Jacobson KA, Moon HR. Discovery of a new nucleoside template for human A₃ adenosine

- receptor ligands: D-4'-thioadenosine derivatives without 4'-hydroxymethyl group as highly potent and selective antagonists. *J. Med. Chem.* 2007; 50: 3159–3162. (b) Jeong, L. S., Pal, S., Choe, S. A., Choi, W. J., Jacobson, K. A., Gao, Z.-G., Klutz, A. M., Hou, X., Kim, H. O., Lee, H. W., Tosh, D. K., Moon, H. R. Structure-activity relationships of truncated D- and L-4'-thioadenosine derivatives as species-independent A₃ adenosine receptor antagonists. *J. Med. Chem.* 2008; 51: 6609–6613. (c) Pal, S., Choi, W. J., Choe, S. A., Heller, C. L., Gao, Z.-G., Chinn, M., Jacobson, K. A., Hou, X., Lee, S. K., Kim, H. O., Jeong, L. S. Structure-activity relationships of truncated adenosine derivatives as highly potent and selective human A₃ adenosine receptor antagonists. *Bioorg. Med. Chem.* 2009; 17: 3733–3738. (d) Jacobson, K. A., Siddiqi, S. M., Olah, M. E., Ji, X. d., Melman, N., Bellamkonda, K., Meshulam, Y., Stiles, G. L., Kim, H. O. Structure-activity relationships of 9-alkyladenine and ribose-modified adenosine derivatives at rat A₃ adenosine receptors. *J Med Chem.* 1995; 38:1720–1735. [PubMed: 7752196]
10. Wang Z, Do CW, Avila MY, Peterson-Yantorno K, Stone RA, Gao ZG, Joshi B, Besada P, Jeong LS, Jacobson KA, Civan MM. Nucleoside-derived antagonists to A₃ adenosine receptors lower mouse intraocular pressure and act across species. *Exp Eye Res.* 2010; 90:146–154. [PubMed: 19878673]
11. Hou X, Kim HO, Alexander V, Kim K, Choi S, Park S, Lee JH, Yoo LS, Gao Z, Jacobson KA, Jeong LS. Discovery of a new human A_{2A} adenosine receptor agonist, truncated 2-hexynyl-4'-thioadenosine. *ACS Med Chem Lett.* 2010; 1:516–520. [PubMed: 21286238]
12. Sitkovsky MV, Lukashev D, Apasov S, Kojima H, Koshiba M, Cladwell C, Ohta A, Thiel M. Physiological control of immune response and inflammatory tissue damage by hypoxia-inducible factors and adenosine A_{2A} receptors. *Ann. Rev. Immunol.* 2004; 22: 657–682. (b) Lappas, C. M., Sullivan, G. W., Linden, J. Adenosine A_{2A} agonists in development for the treatment of inflammation. *Expert Opin Invest Drugs.* 2005; 14:797–806.
13. (a) Kato K, Hayakawa H, Tanaka H, Kumamoto H, Shindoh S, Shuto S, Miyasaka T. A new entry to 2-substituted purine nucleosides based on lithiation-mediated stannyl transfer of 6-chloropurine nucleosides. *J Org Chem.* 1997; 62:6833–6841. (b) Brun V, Legraverend M, Grierson DS. Cyclin-dependent kinase (CDK) inhibitors: development of a general strategy for the construction of 2,6,9-trisubstituted purine libraries. Part 1. *Tetrahedron Lett.* 2001; 42:8161–8164. (c) Taddei D, Kilian P, Slawin AMZ, Woollins D. Synthesis and full characterization of 6-chloro-2-iodopurine, a template for the functionalisation of purines. *Org Biomol Chem.* 2004; 2:665–670. [PubMed: 14985806]
14. Chinchilla R, Nájera C. The Sonogashira reaction: A booming methodology in synthetic organic chemistry. *Chem Rev.* 2007; 107:874–922. [PubMed: 17305399]
15. Suzuki A. Carbon-carbon bonding made easy. *Chem Commun.* 2005; 38:4759–4763.
16. Miyaura N, Suzuki A. Palladium-catalyzed reaction of 1-alkenylboronates with vinylic halides: (1Z,3E)-1-phenyl-1,3-octadiene. *Org Syn Coll Vol.* 1993; 8:532–534.
17. Laxer A, Major DT, Gottlieb HE, Fischer B. (¹⁵N₅)-Labeled adenine derivatives: Synthesis Studies of Tautomerism by ¹⁵N NMR Spectroscopy Theoretical Calculations. *J Org Chem.* 2001; 66:5463–5481. [PubMed: 11485471]
18. (a) Perreira M, Jiang JK, Klutz AM, Gao ZG, Shainberg A, Lu C, Thomas CJ, Jacobson KA. Reversine and its 2-substituted adenine derivatives as potent and selective A₃ adenosine receptor antagonists. *J Med Chem.* 2005; 48:4910–4918. [PubMed: 16033270] (b) Jarvis MF, Schutz R, Hutchison AJ, Do E, Sills MA, Williams M. [³H]CGS 21680 a selective A₂ adenosine receptor agonist directly labels A₂ receptors in rat brain. *J Pharmacol Exp Ther.* 1989; 251:888–893. [PubMed: 2600819] (c) Olah ME, Gallo-Rodriguez C, Jacobson KA, Stiles GL. ¹²⁵I-4-Aminobenzyl-5'-N-methylcarboxamidoadenosine a high affinity radioligand for the rat A₃ adenosine receptor. *Mol Pharmacol.* 1994; 45:978–982. [PubMed: 8190112] (d) Nordstedt C, Fredholm BB. A modification of a protein-binding method for rapid quantification of cAMP in cell-culture supernatants and body fluid. *Anal Biochem.* 1990; 189:231–234. [PubMed: 2177960]
19. (a) Matsuda A, Shinozaki M, Yamaguchi T, Homma H, Nomoto R, Miyasaka T, Watanabe Y, Abiru T. 2-Alkynyladenosines: a novel class of selective adenosine A₂ receptor agonists with potent antihypertensive effects. *J Med Chem.* 1992; 35:241–252. [PubMed: 1732541] (b) Cristalli G, Volpini R, Vittori S, Camaioni E, Monopoli A, Conti A, Dionisotti S, Zocchi C, Ongini E. 2-Alkynyl derivatives of adenosine-5'-N-ethyluronamide (NECA): selective A₂ adenosine receptor agonists with potent inhibitory activity on platelet aggregation. *J Med Chem.* 1994; 37:1720–1726.

- [PubMed: 8201607] (c) Lambertucci C, Costanzi S, Vittori S, Volpini R, Cristalli G. Synthesis and adenosine receptor affinity and potency of 8-alkynyl derivatives of adenosine. *Nucleosides, Nucleotides & Nucleic Acids*. 2001; 20:1153–1157.
20. Bevan N, Butchers PR, Cousins R, Coates J, Edgar EV, Morrison V, Sheehan MJ, Reeves J, Wilson DJ. Pharmacological characterisation and inhibitory effects of (2R,3R,4S,5R)-2-(6-amino-2-[[[(1S)-2-hydroxy-1-(phenylmethyl)ethyl]amino]-9H-purin-9-yl]-5-(2-ethyl-2H-tetrazol-5-yl)]tetrahydro-3,4-furandiol, a novel ligand that demonstrates both adenosine A_{2A} receptor agonist and adenosine A₃ receptor antagonist activity. *Eur J Pharmacol*. 2007; 564:219–225. [PubMed: 17382926]
 21. Morris CJ. Carrageenan-induced paw edema in the rat and mouse. *Methods Mol Biol*. 2003; 225:115–121. [PubMed: 12769480]
 22. Otterness IG, Moore PF. Carrageenan foot edema test. *Methods Enzymol*. 1988; 162:320–327. [PubMed: 3226312]
 23. Jaakola VP, Griffith MT, Hanson MA, Cherezov V, Chien EYT, Lane JR, IJzerman AP, Stevens RC. The 2.6 Å crystal structure of a human A_{2A} adenosine receptor bound to an antagonist. *Science*. 2008; 322:1211–1217. [PubMed: 18832607]
 24. Bradford MM. A rapid and sensitive method for the quantitation of microgram quantities of protein utilizing the principle of protein-dye binding. *Anal Biochem*. 1976; 72:248–254. [PubMed: 942051]
 25. Kecskés A, Tosh DK, Wei Q, Gao ZG, Jacobson KA. GPCR ligand dendrimer (GLiDe) conjugates: Adenosine receptor interactions of a series of multivalent xanthine antagonists. *Bioconjugate Chem*. 2011; 22:1115–1127.
 26. Jarvis MF, Schutz R, Hutchison AJ, Do E, Sills MA, Williams MJ. [³H]CGS 21680, a selective A₂ adenosine receptor agonist directly labels A₂ receptors in rat brain. *Pharmacol Exp Ther*. 1989; 251:888–893.
 27. Olah ME, Gallo-Rodriguez C, Jacobson KA, Stiles GL. ¹²⁵I-4-aminobenzyl-5'-N-methylcarboxamidoadenosine, a high affinity radioligand for the rat A₃ adenosine receptor. *Mol Pharmacol*. 1994; 45:978–982. [PubMed: 8190112]
 28. (a) Nordstedt C, Fredholm BB. A modification of a protein-binding method for rapid quantification of cAMP in cell-culture supernatants and body fluid. *Anal Biochem*. 1990; 189:231–234. [PubMed: 2177960] (b) Post SR, Ostrom RS, Insel PA. Biochemical methods for detection and measurement of cyclic AMP and adenylyl cyclase activity. *Methods Mol Biol*. 2000; 126:363–374. [PubMed: 10685423]
 29. Cheng YC, Prusoff HR. Relationship between the inhibition constant (K₁) and the concentration of inhibitor which causes 50 per cent inhibition (I₅₀) of an enzymatic reaction. *Biochem Pharmacol*. 1973; 22:3099–3108. [PubMed: 4202581]
 30. Yeşilada E, Küpeli E. Berberis crataegina DC. root exhibits potent anti-inflammatory, analgesic and febrifuge effects in mice and rats. *J Ethnopharmacol*. 2002; 79:237–248. [PubMed: 11801387]

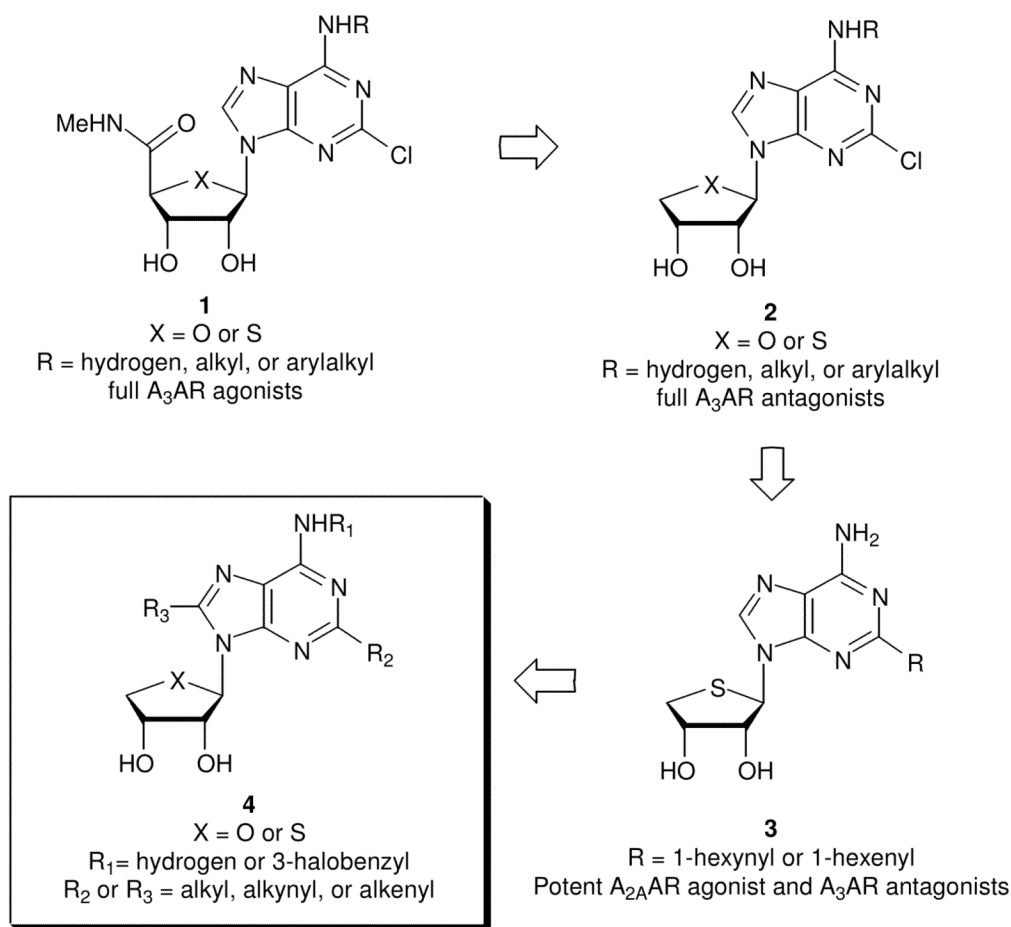


Figure 1.

The design of the target nucleosides acting dually at the A_{2A} and A₃ARs. A molecular modeling study⁸ indicated that the NH of the 5'-uronamide of **1** serves as a hydrogen bonding donor in the A₃AR binding site and is associated with the induced fit for the receptor activation. On this basis, we designed and synthesized truncated adenosine derivatives **2**⁹ removing the 5'-uronamide of **1**, to bind potently but with altered ability to induce the conformational change essential for receptor activation. As expected, members of the series of compound **2** proved to be potent and selective A₃AR antagonists.⁹ It should be noted that these A₃AR antagonists **2** also showed species-independent binding affinity, making them suitable for efficacy evaluation for drug development in small animal models.⁹ Compound **2** (X = S, R = 3-iodobenzyl) exhibited a potent anti-glaucoma effect in vivo.¹⁰

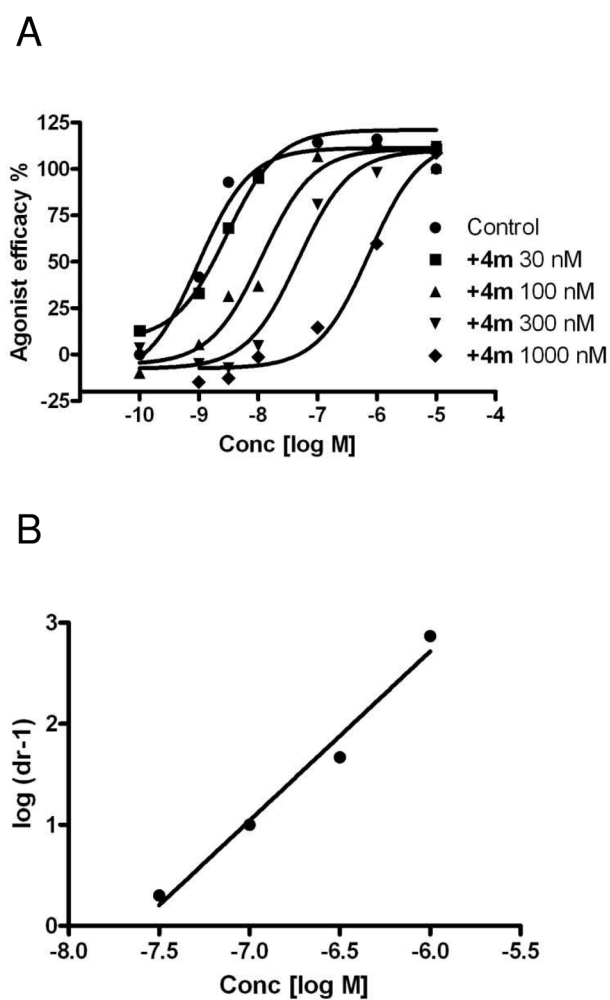


Figure 2. Effects of compound **4m** on inhibition of cAMP production induced by full agonist **1a** at the hA₃AR expressed in CHO cells (A). The data was transformed to a linear Schild plot (B) indicating competitive antagonism with a K_B value of 23.9 nM.

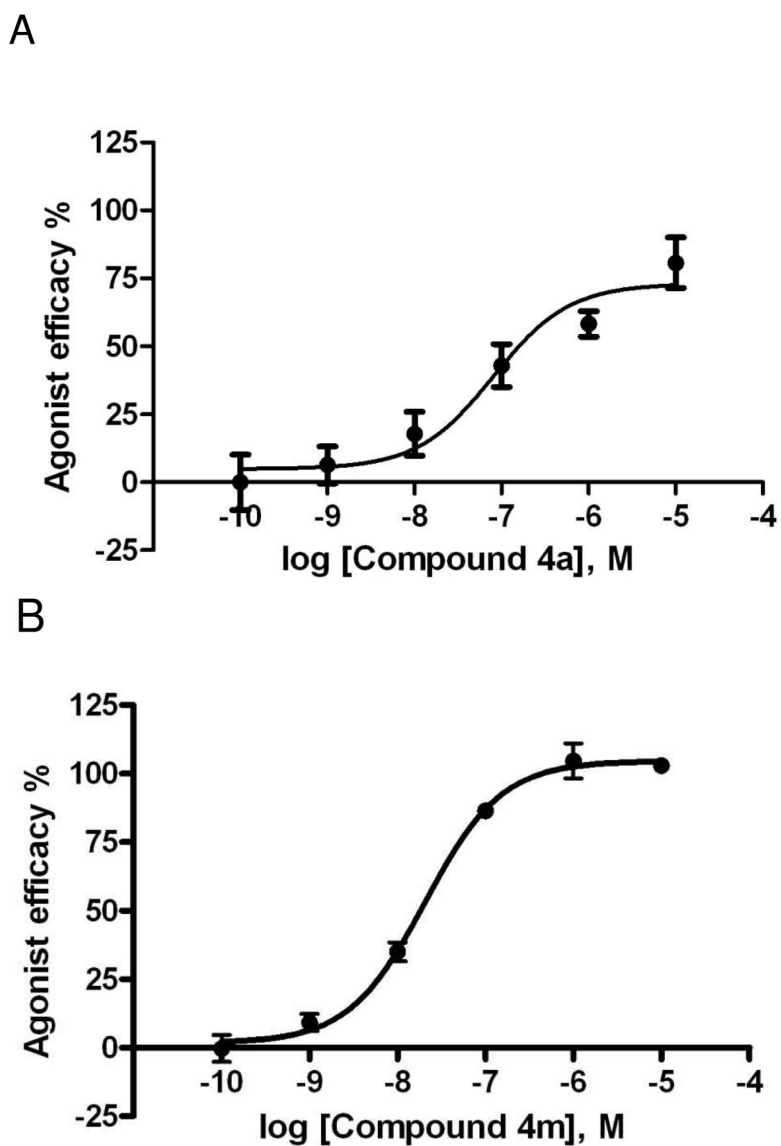


Figure 3. Effects of compounds **4a** (A) and **4m** (B) in stimulation of cAMP production at the hA_{2A}AR expressed in CHO cells, compared to NECA as reference full agonist (= 100%).

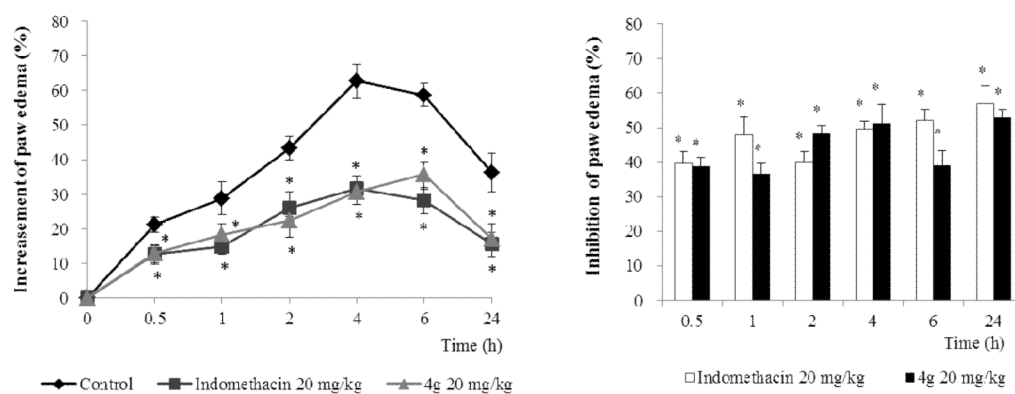


Figure 4. Inhibitory effect of **4g** on the carrageenan-induced paw edema. Paw edema was induced as described in the Experimental Section. The paw volume was measured before (0 h) and at intervals of 0.5, 1, 2, 4, 6 and 24 h after carrageenan injection using a plethysmometer. Data represent the mean \pm S.D. (n=6). *indicates statistically significant differences from the control group ($P < 0.01$).

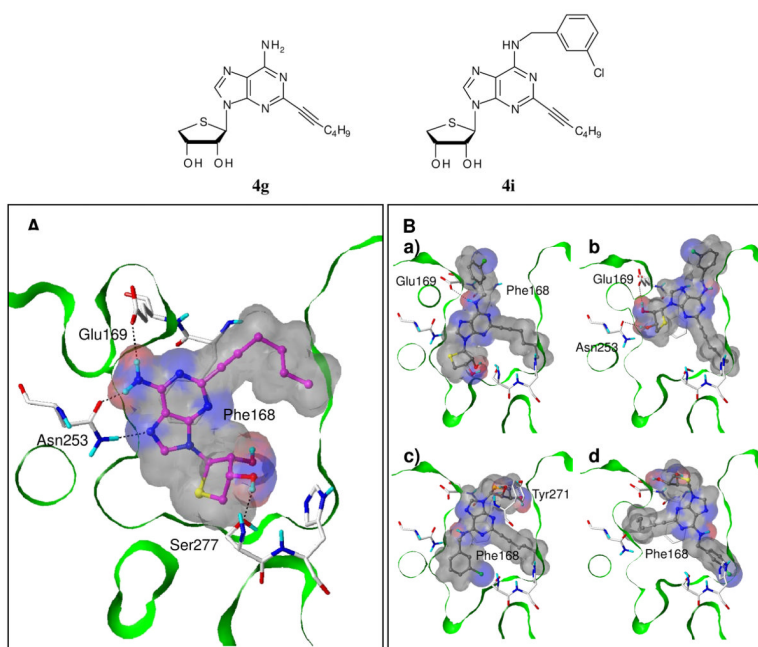


Figure 5. Predicted binding modes of the C2-substituted derivative **4g** and its N^6 -chlorobenzyl derivative **4i** in an $A_{2A}AR$ crystal structure.²³ (A) Compound **4g** binds very well to the receptor, interacting with important residues at the binding site. (B) Compound **4i** shows various binding modes and does not maintain the key interactions. Compounds **4g** and **4i** are depicted in ball-and-stick with carbon atoms in magenta and gray, respectively. The key residues are displayed as capped-stick with carbon atoms in white, and the hydrogen bonds are marked in black dashed lines. The van der Waals surfaces of the ligands are colored by hydrogen bonding capability (red: H-bond donating region; blue: H-bond accepting region). The Fast Connolly surface of the protein is Z-clipped, and the non-polar hydrogens are undisplayed for clarity.

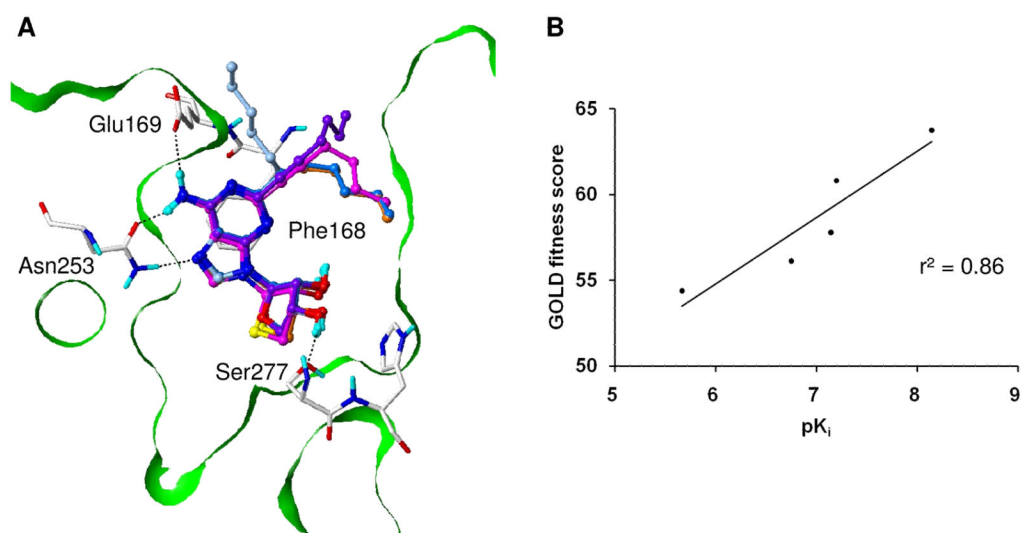
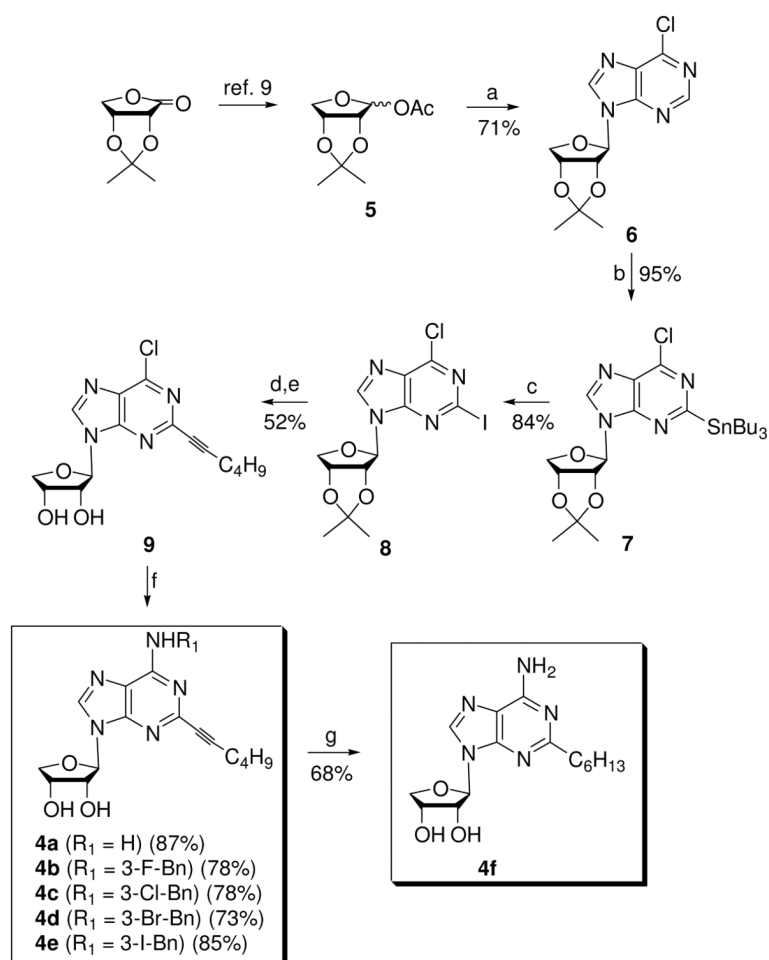
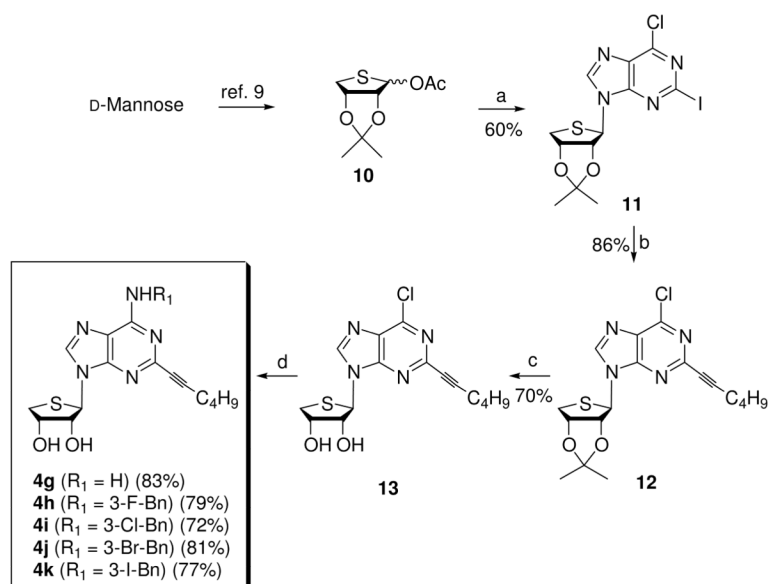


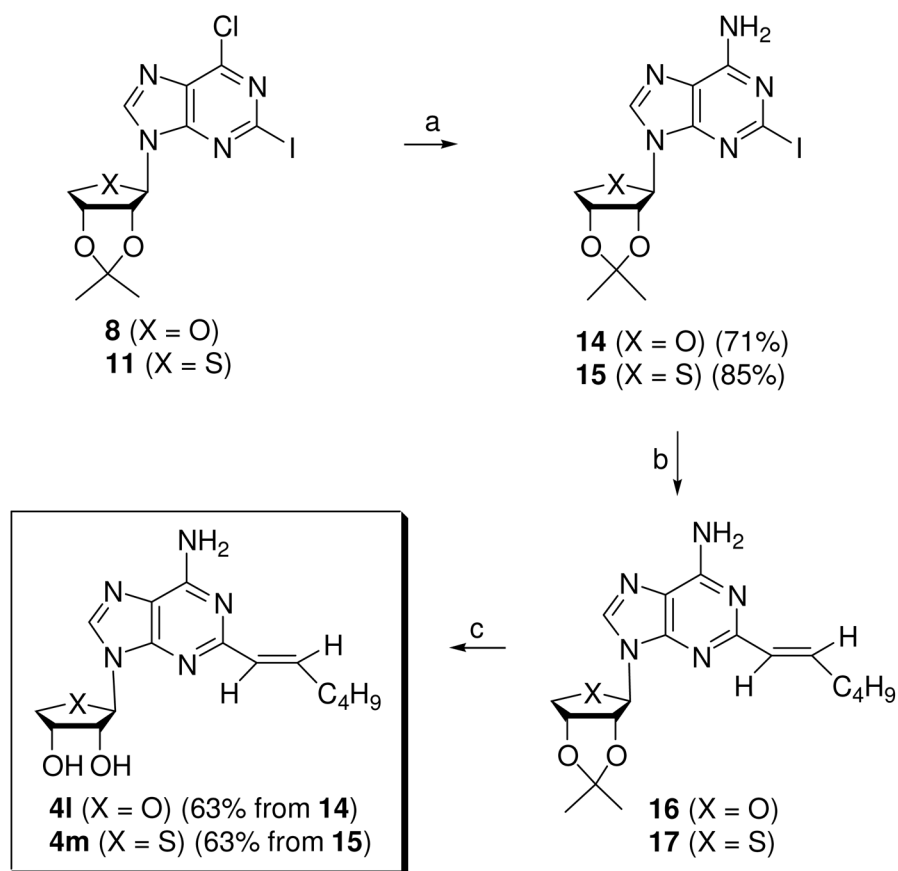
Figure 6. Predicted binding modes of the five C₂-substituted and N⁶-unsubstituted derivatives in an hA_{2A}AR crystal structure,²³ and the correlation between their experimental binding affinities and docking scores. (A) The adenine and sugar moieties of the molecules showed almost exactly the same binding modes maintaining the key interactions. Compounds **4a**, **4f**, **4g**, **4l**, and **4m** are depicted as ball-and-stick with carbon atoms in purple, light-blue, magenta, skyblue and orange, respectively. (B) The scatter plot of the pK_i values and GOLD fitness scores for the five compounds showed a good correlation with r² of 0.86.

**Scheme 1^a**

Reagents and conditions^a: a) silylated 6-chloropurine, TMSOTf, DCE, rt to 80 °C, 5 h; b) LiTMP, Bu₃SnCl, THF, hexane, -78 °C, 1 h; c) I₂, THF, rt, 24 h; d) 1-hexyne, Cs₂CO₃, (Ph₃P)₄Pd, CuI, DMF, rt, 3 h; e) 1 N HCl, THF, rt, 15 h; f) NH₃/*t*-BuOH, 100 °C, 8 h or R₁NH₂, Et₃N, EtOH, rt, 24–48 h; g) Pd/C, H₂, MeOH.

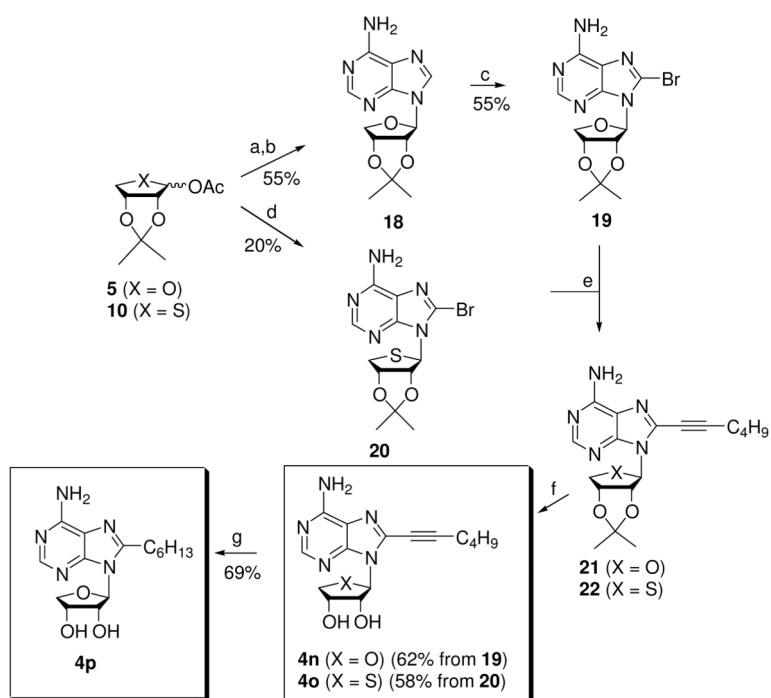
**Scheme 2^a**

Reagents and conditions^a: a) 2-iodo-6-chloropurine, BSA, TMSOTf, CH₃CN, rt to 80 °C, 3 h; b) 1-hexyne, Cs₂CO₃, (Ph₃P)₄Pd, CuI, DMF, rt, 3 h; c) 1 *N* HCl, THF, rt, 20 h; d) NH₃ in *t*-BuOH, 100 °C, 8 h or R₁NH₂, Et₃N, EtOH, rt, 48 h.

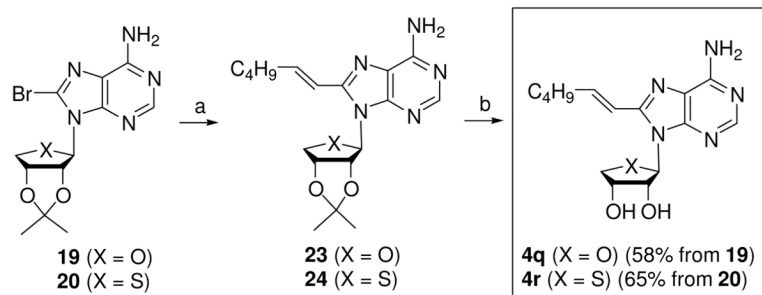


Scheme 3^a

Reagents and conditions^a: a) NH_3/MeOH , 80 °C, 2 h; b) (*E*)-1-catecholboranylhexene, $(\text{Ph}_3\text{P})_4\text{Pd}$, Na_2CO_3 , DMF, H_2O , 90 °C, 15 h; c) 1 *N* HCl, THF, rt, 15 h.

**Scheme 4^a**

Reagents and conditions^a: a) silylated 6-chloropurine, TMSOTf, DCE, rt to 80 °C, 5 h; b) NH₃, MeOH, 80 °C, 2 h; c) Br₂, 1 N NaOAc, MeOH, rt, 40 min; d) silylated 8-bromoadenine, TMSOTf, DCE, rt to 90 °C, 2 h; e) 1-hexyne, CuI, TEA, DMF, (PPh₃)₂PdCl₂, rt, 3 h; f) 1 N HCl, THF, rt, 15 h; g) H₂, Pd/C, MeOH, 15 h.

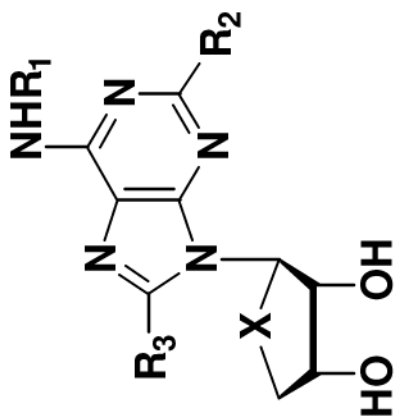
**Scheme 5^a**

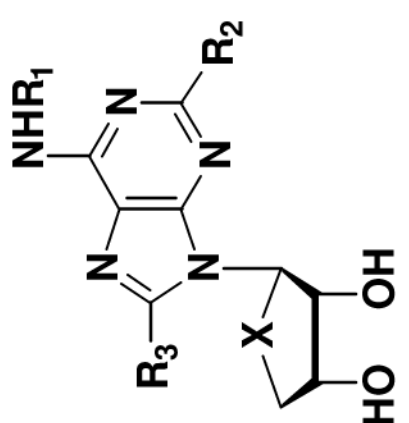
Reagents and conditions^a: a) (*E*)-1-catecholboranylhexene, $(\text{Ph}_3\text{P})_4\text{Pd}$, Na_2CO_3 , DMF, H_2O , $90\text{ }^\circ\text{C}$, 15 h; b) 1 *N* HCl, THF, rt, 15 h.

Table 1

Binding affinities of known A₃AR antagonist **2** and truncated C2- and C8-substituted derivatives **4a–4r** at three subtypes of hARs and A₃AR-mediated inhibition of cAMP production

Compounds (R ₁ , R ₂ , R ₃)	Affinity (K _d , nM ± SEM, or % inhibition) ^a			Relative efficacy (%inhibition of cAMP ± SEM) ^c	
	hA ₁	hA _{2A}	hA ₃	hA ₃	hA ₃
2 (X = S, R ₁ = 3- <i>I</i> -Bn, R ₂ = Cl, R ₃ = H) ^b	2490 ± 940	341 ± 75	4.16 ± 0.50	4.2 ± 2.3	
4a (X = O, R ₁ = H, R ₂ = 2-hexynyl, R ₃ = H)	740 ± 430	63.2 ± 15	138 ± 44	17.4 ± 2.4	
4b (X = O, R ₁ = 3- <i>F</i> -Bn, R ₂ = 2-hexynyl, R ₃ = H)	9 ± 1%	25 ± 3%	570 ± 130	29.5 ± 5.5	
4c (X = O, R ₁ = 3- <i>Cl</i> -Bn, R ₂ = 2-hexynyl, R ₃ = H)	9 ± 5%	42 ± 13%	150 ± 140	39.7 ± 3.8	
4d (X = O, R ₁ = 3- <i>Br</i> -Bn, R ₂ = 2-hexynyl, R ₃ = H)	12 ± 4%	27 ± 4%	67 ± 18	37.2 ± 2.9	
4e (X = O, R ₁ = 3- <i>I</i> -Bn, R ₂ = 2-hexynyl, R ₃ = H)	18 ± 2%	32 ± 9%	220 ± 50	31.5 ± 2.8	
4f (X = O, R ₁ = H, R ₂ = 2-hexynyl, R ₃ = H)	10 ± 5%	2160 ± 270	39 ± 5%	22.3 ± 4.5	
4g (X = S, R ₁ = H, R ₂ = 2-hexynyl, R ₃ = H)	39 ± 10%	7.19 ± 0.6	11.8 ± 1.3	2.8 ± 1.6	
4h (X = S, R ₁ = 3- <i>F</i> -Bn, R ₂ = 2-hexynyl, R ₃ = H)	24 ± 5%	46 ± 5%	150 ± 80	47.6 ± 4.9	
4i (X = S, R ₁ = 3- <i>Cl</i> -Bn, R ₂ = 2-hexynyl, R ₃ = H)	25 ± 2%	3730 ± 200	24.0 ± 6.0	47.2 ± 3.4	
4j (X = S, R ₁ = 3- <i>Br</i> -Bn, R ₂ = 2-hexynyl, R ₃ = H)	12 ± 1%	3910 ± 970	24.0 ± 5.0	25.2 ± 3.0	
4k (X = S, R ₁ = 3- <i>I</i> -Bn, R ₂ = 2-hexynyl, R ₃ = H)	15 ± 3%	4890 ± 840	39 ± 5	40.0 ± 5.6	
4l (X = O, R ₁ = H, R ₂ = 2-hexynyl, R ₃ = H)	31.9 ± 1.2%	178 ± 26	218 ± 79	42.6 ± 3.1	





Compounds (R ₁ , R ₂ , R ₃)	Affinity (K _i , nM ± SEM, or % inhibition) ^a			Relative efficacy (%inhibition of cAMP ± SEM) ^c
	hA ₁	hA _{2A}	hA ₃	
4m (X = S, R ₁ = H, R ₂ = 2-hexenyl, R ₃ = H)	16.2 ± 8.4%	72.0 ± 19.1	13.2 ± 0.8	10.7 ± 4.1
4n (X = O, R ₁ = H, R ₂ = H, R ₃ = 2-hexynyl)	290 ± 70	27.2 ± 2.9%	31.7 ± 7.4	24.5 ± 2.9
4o (X = S, R ₁ = H, R ₂ = H, R ₃ = 2-hexenyl)	49.3 ± 4.9%	46.5 ± 4.3%	20.0 ± 4.0	1.7 ± 3.9
4p (X = O, R ₁ = H, R ₂ = H, R ₃ = 2-hexenyl)	18.1 ± 5.0%	5.8 ± 4.6%	24.7 ± 2.1%	12.9 ± 2.2
4q (X = O, R ₁ = H, R ₂ = H, R ₃ = 2-hexenyl)	500 ± 140	27.3 ± 6.3%	94.2 ± 30.0	19.5 ± 2.4
4r (X = S, R ₁ = H, R ₂ = H, R ₃ = 2-hexenyl)	3.7 ± 2.9%	22.8 ± 6.4%	259 ± 10	6.1 ± 1.7

^aAll binding experiments were performed using adherent mammalian cells stably transfected with cDNA encoding the appropriate hAR (A₁AR and A₃AR in CHO cells and A_{2A}AR in HEK-293 cells). Binding was carried out using 1 nM [³H]-R-(+)-N6-2-phenylisopropyl adenosine (R-PIA), [³H]-2-[p-(2-carboxyethyl)phenyl-ethylamino]-5'-N-ethylcarboxamidoadenosine (**26**, CGS21680, 10 nM), or 0.5 nM [¹²⁵I]-N⁶-(3-iodo-4-aminobenzyl)-5'-N-methylcarboxamidoadenosine (**27**, I-AB-MECA) as radioligands for A₁, A_{2A}, and A₃ARs, respectively. Values are expressed as mean ± sem, n = 3–4 (outliers eliminated) and normalized against a non-specific binder **25** (10 μM). Values expressed as a percentage in italics refer to percent inhibition of specific radioligand binding at 10 μM, with nonspecific binding defined using 10 μM **25**.

^bRef. 1.

^cMaximal efficacy (at 10 μM) in an A₃AR functional assay, determined by inhibition of forskolin-stimulated cAMP production in AR-transfected CHO cells, expressed as percent inhibition (mean ± standard error, n = 3–5) in comparison to effect (100%) of full agonist **1a** at 10 μM.

^dData for compounds **4g**, **4m**, **4o**, and **4r** are from reference 11